TECHNISCHE
UNIVERSITÄT
WIEN

Institut für
Computertechnik
Institute of
Computer Technology

Master's Thesis

submitted by

Philipp Schlögl, BSc.

An Energy Harvesting Powered Sensor Node for Machine Condition Monitoring

In partial fulfillment of the requirements for the degree of

Master of Science (MSc)

Vienna, Austria, 2018

Study code:	066 504
Field of study:	Embedded Systems

Supervisor:	Univ.Prof. Dipl.-Ing. Dr.techn. Axel Jantsch
Co-Supervisor:	Univ.Ass. Dipl.-Ing. Dr.techn. Michael Rathmair

Abstract

Monitoring the condition of machines is a long-used approach to keep the machine in a safe state. Observing oil pressure, oil temperature or rotating speed are general examples for it. Since at rotating parts oscillations always occur, vibration analysis is a widely used approach to monitor the condition of a machine [MTPP12] [HVD$^+$15] [SK17]. Even at the best produced machine vibration appears because of mechanical tolerances which cannot be avoided [KV86]. Due to the evolution in the electronic industry there are several sensor types available which can be used to monitor the vibration of a machine. In this work a wireless self-powered sensor node is developed which measures the vibration of a machine and provides the data to an analysis computer. The know-how about the condition of machines allows planning maintenance if the need arises. Surprising faults which lead to a long downtime of the machine or even to a catastrophic crash where the machine can be damaged, or humans can be injured can be avoided. If one or more indicator show that the performance of a machine is decreasing or that the machine is going to fail maintenance can be performed [SJ15]. This type of maintenance is called Condition-based Maintenance (CbM) [Ran11]. The developed sensor node is self-powered with a thermoelectric generator (TEG). Because of the temperature difference of the warm machine surface and the colder surrounding electric energy can be produced [43]. The control unit of the sensor node is a microcontroller which controls the activities on the node and transmits the measured sensor data via Bluetooth Low Energy (BLE) chip to an analysis device which performs further analysis of the current machine condition or future trend analysis.

Kurzfassung

Die Zustandsüberwachung von Maschinen ist ein schon lange praktizierter Ansatz, um die Maschine in einem sicheren Betriebszustand zu betreiben. Die Kontrolle des Öldrucks, der Öltemperatur oder der Drehzahl sind allgemeine Beispiele dafür. Da bei rotierenden Teilen immer Schwingungen auftreten, ist die Vibrationsanalyse eine weit verbreitete Vorgehensweise, um den Zustand einer Maschine zu überwachen [MTPP12] [HVD+15] [SK17]. Sogar bei präzise hergestellten Maschinen treten Vibrationen aufgrund von unvermeidbaren mechanischen Toleranzen auf [KV86]. Durch die Entwicklung in der Elektronikindustrie sind verschiedene Sensortypen verfügbar, die für die Zustandsüberwachung eingesetzt werden können. Im Zuge dieser Arbeit wurde ein drahtloser Sensorknoten entwickelt, welcher in der Lage ist, die Vibration einer Maschine zu messen und die Daten einem Analysegerät zur Verfügung zu stellen. Das Wissen über den Zustand einer Maschine erlaubt eine genau Planung von Wartungsarbeiten, wenn sie erforderlich sind. Des Weiteren können überraschende Fehler, welche zu langen Ausfallzeiten der Maschine oder sogar zur Beschädigung dieser oder zu Verletzungen von Personal führen, vermieden werden. Melden ein oder mehrere Sensoren, dass die Leistung der Maschine nachlässt oder die Maschine in einem Fehlerzustand ist, können Reparaturarbeiten durchgeführt werden [SJ15]. Diese Art von Wartung wird zustandsabhängige Wartung genannt [Ran11]. Der entwickelte Sensorknoten wird von einem Thermoelektrischen Generator (TEG) mit elektrischer Energie versorgt. Dieser kann durch den Temperaturunterschied der warmen Oberfläche der Maschine und der kühleren Umgebung elektrische Energie erzeugen [43]. Die Steuereinheit des Sensors ist ein Mikrokontroller, welcher die Aktivitäten steuert und die gemessenen Sensordaten mithilfe eines Bluetooth Low Energy (BLE) Bausteins weitersendet. Die Daten können für eine Analyse des aktuellen Zustands der Maschine aber auch für eine Trendanalyse für den zukünftigen Zustand verwendet werden.

Acknowledgements

First I would like to thank Prof. Axel Jantsch of the Institute of Computer Technology at the TU Wien for supervising my master thesis. I would also like to thank my supervisor Michael Rathmair for his support and advice during my thesis. The door to his office was always open and he was always willing to help me.

I would like to thank all my colleagues at *Analog Devices, Inc.* who answered all my questions, helped me with my problems and made working on my thesis a great experience. A special thanks to Mike Heffernan and Christopher Murphy who made my master thesis in cooperation with *Analog Devices, Inc.* possible. I learned a lot during this time and I am grateful for this opportunity.

Last but not least I would like to thank my girlfriend, my parents and my sister for supporting me the whole time during my studies.

Table of Contents

1 Introduction

To achieve maximum operating time for a machine, the equipment was originally designed for "run to break" with the effect that breakdowns could be catastrophic. The volume of damage can be increased because components which are in good condition or connected machines can also be damaged through such failure. This results in increased time and costs of repairing and higher production loss through the unpredictable shutdown. To overcome this drawback maintenance can be done in regular intervals, so-called preventive maintenance. The interval is chosen to be shorter than the expected "time between failures" so that just a small amount of equipment would fail. The given time interval allows a well planned and fast maintenance. The disadvantage of this strategy is that the majority of machines could have stayed in operation for a much longer time and that maintenance personnel often replace good parts during the maintenance. This increases the use of spare parts and maintenance work. Because of the "infant mortality" of the new installed parts, failures could happen which wouldn't have happened without maintenance when the proven parts would have kept in operation. Condition-based maintenance, also called predictive maintenance, overcomes the disadvantages of preventive maintenance. Sensors measure the condition of machines and the cause of a failure can be analysed or a prognosis of the remaining lifetime can be predicted. If the need of maintenance arises it can be planned and performed at the optimum time [Ran11].

This work is structured as follows: This section is about benefits of condition-based maintenance, problems of existing condition monitoring systems and the goal of this thesis. Section II describes the state of the art followed by a description of the design approach of the developed system in Section III and a discussion of the results in Section IV. This work is concluded by an explanation of potential future work and a conclusion.

1.1 Motivation for Condition-based Maintenance

Condition-based Maintenance (CbM) is an approach where maintenance is performed when the need arises. Contrary to this is the philosophy of preventative maintenance where maintenance is done periodically even if there is no need for it. In [AAB16] condition maintenance is summarized as a process which focuses on fault or failure detection with the goal of minimizing downtime and also operating and maintenance costs to maximize the production. Advantages of a CbM system are [Gol99] [SJ15]:

- Reducing unscheduled down time

- Required maintenance can be planned and resources can be requested

- Elimination of periodic disassembly of machine for inspection

- Greatly reduced probability of machine "crash"

- Minimizing the need of a present technician to identify the cause of error

Reducing unscheduled down time by planned maintenance: If indications of a possible failure of a machine arise, maintenance can be scheduled during a practical time, for example during a planned shutdown. Required replacement parts, tools and equipment can be prepared and the maintenance stuff can be requested to minimize the time and costs of the maintenance. Well planned repairing procedures of a machine reduces the maintenance cost and minimize the production lost while the machine is under maintenance and has to be stopped [Gol99] [SJ15] [COV+18].

Elimination of periodic disassembly: To check the condition of bearings, gearboxes or whole machines technicians can disassemble the equipment periodically. If a broken part is found during the inspection, it is replaced by a new part. Often all critical parts and also good ones, get replaced by new parts because the machine is already disassembled. This leads to a higher risk of a failure after the maintenance because parts which are in good condition and could stay longer in operation could be replaced by parts with material faults or other defects. The failure distribution of material, electronic or mechanic components, in general called bathtub curve, shows the fail rate as a function of lifetime, see Figure 1.1. The observed failure rate is higher at the beginning because of material defects or other faults and gets lower during the lifetime where random failures are dominant. Broken bearings have been detected in wind power plants after three years which is about five to ten percent of the calculated lifetime of such bearings [27]. When the component's lifetime gets closer to the maximum lifetime the failure rate gets higher because of wear-out failures [FHT11]. Often disassembling and reassembling increases the chance that the machines is not assembled properly or that something is mounted wrong [Gol99] [SJ15].
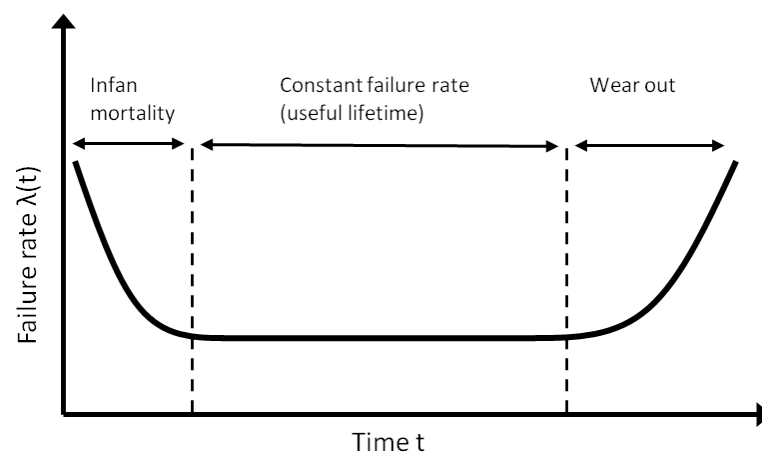

Figure 1.1: Bathtub curve of failure rate. Source: [XWJ08]

Avoiding machine crash: Keeping the machine in operation until total destruction is dangerous and uneconomical. The maintenance costs are lower when maintenance is performed

in time because the probability of a fast repair is higher when the machine is not running until crash so that only broken parts need to be replaced instead of replacing the whole machine. It could also be possible that operating personnel is near the machine when it totally destructs and this can cause injury or even death [Gol99].

Minimizing the need of a present technician: Without an automatic condition monitoring system the condition of the machines must be checked by a technician from time to time, this can be done with hand-held vibration meters or other tools [20] [5]. Critical machines need to be monitored in shorter time intervals because a breakdown leads to dangerous or costly consequences. The manual checking of the machines is very time consuming and therefore the costs are higher. Monitoring a running machine or equipment that is in a hazardous environment is an additional risk for the maintenance personnel. The hand-held devices are held to the machine or bearing housing with a weak coupling between the machine and the analysis device and therefore these devices have a lower frequency range. In this case the sensor is not mounted to the machine as good as it would be with a screw or a magnet. It is not recommended to measure vibrations with frequency above 1 kHz with handheld devices, so therefore machine faults which produce frequencies above the measurement range might stay undetected [13] [iso02].

Cost savings by Condition-based Maintenance

This section describes some examples of how beneficial a CbM system is in the industry. In [30] a cost saving potential for CbM solution for wind turbines is compared to planned maintenance. Oil changes are done when they are needed and brings cost savings of about 40.000 € over a ten year period, this values scales up quickly for a wind farm with many wind power plants. In [25] the costs of an up-tower and a down-tower repair of a generator and a gearbox from a wind power plant are compared. If a CbM system is installed and warns of an upcoming machine fault an up-tower repair can be performed which is about 43.500 € (50.000 $). If the equipment breaks down without warning a crane is needed to drop and re-install it after the repair. The costs of a new generator or gearbox are about 218.000 € (250.000 $) and the costs of renting a crane is about 130.000 € (150.000 $). An installed CbM system in a manufacturing site in Spain of a paper company brings cost savings in maintenance of about 250.000€ every year and allows a ten percent production growth [34]. Condition monitoring of a gearbox from an industrial mill allows an early repair and no production loss due to a scheduled shut down, the estimated cost savings from doing this are 278.500 €. An early replacement of a pump bearing avoids damage to the pump and brings estimated cost savings of 44.500 €, also an early replacement of the roller bearing and mechanical seal could avoid extensive damage and brings estimated cost savings of 30.000 € [8].

1.2 Problem Definition

Monitoring and analysing the condition of a machine is an important task to keep it in good condition, to extend the lifetime of a machine and to guarantee the quality in production lines. Nowadays companies focus on reducing the costs of their products. The selling price of their products has to cover the production costs and it must be profitable. As the production costs also include the costs of a CbM system, the CbM system has to be cost effective. Most available CbM systems are battery powered and thus have a limited lifetime [22] [19] [4] [Inc13] [16][SW17]. Once the battery is empty or at a low level the battery needs to be replaced or charged which requires

human intervention [WBV$^+$11] [CC08]. This is time consuming and leads to high maintenance costs. CbM systems are often placed in a dangerous environment or they are hard to reach and might require a stop of the machine. The batteries might contain toxic chemicals and could impact the environment when incorrectly disposed [SS09] [26]. To avoid the disadvantages of batteries an energy harvesting solution is proposed. Energy from the environment is converted to electric energy and is used to power the condition monitoring system. The following items list the main benefits of an energy harvesting solution for powering condition monitoring systems:

- Avoiding the environmental impact from the toxic chemicals in batteries

- Eliminating the time and cost consuming replacement of batteries

- Maintenance personnel is not in a dangerous area for battery replacement

Batteries and their impact to the environment: Every year two million batteries are collected by the waste management of Vienna and the usage of batteries increases every year [6]. Used batteries are classified as problem material because batteries contain dangerous and toxic chemicals and can harm the environment. Lithium for example is highly reactive and can cause heavy chemical reactions, fire or explosions when it gets in contact with water or air. Improperly disposed batteries can pollute the air, the water and the soil with its toxic materials [6] [12] [42] [7]. Another drawback of batteries is the very energy-intensive recycling process of batteries, it takes about six to ten times more energy to reclaim metal from used batteries as it would take by mining [EnO15]. An important raw material for the production of lithium batteries is cobalt. More than half of the worldwide mined cobalt is mined in Democratic Republic of the Congo and about 20 percent of it is done by hand. Amnesty International documented that cobalt mining in the Democratic Republic of the Congo is linked with child labour and in 2016 Amnesty International documented that children and adults were mining cobalt in small, handmade tunnels while risking their lives. Further investigation showed that the battery producer didn't know about their supply chain and the working conditions in cobalt mines and that the awareness for this situation slowly increases [36]. The Production, transportation and distribution of batteries is very energy consuming and consumes natural resources. Using rechargeable batteries would decrease the usage of these resources and avoid the production of new batteries as the same battery can be used after recharging [41]. Using energy harvesting solutions can be compared with rechargeable batteries as the energy harvesters have to be produced, transported and distributed but the follow-up costs are less because the energy harvesting solution doesn't need a replacement or recharge process.

Costs of battery replacement in a wireless sensor systems: The following examples show the costly and time-consuming process of battery replacement and the benefit of an energy harvesting solution for the wireless sensor node: In [Tec08] the costs of battery replacement are estimated at 70-435 € (80-500 $) per wireless device. In [44] a battery replacement is calculated at 220 € (250$) while six to eight batteries are needed for a sensor node during its lifetime. The costs multiplied by 500 devices results in the total battery maintenance costs of 653.000 € (750.000 $) for 3.000 batteries. In [23] the personnel costs for battery replacement in wireless sensor applications is predicted to be more than one billion dollars over the next few years. An example in [EnO15] shows total battery maintenance costs of 19,60 € (22,5 $) when 3 battery replacements are done during a 20-year sensor node lifetime. Another example shows that 30 battery replacements could be required per day, in a

large system consisting of 10.000 wireless sensor nodes each sensor node being powered by a battery that has a two year-lifetime [EnO15]. In [24] the costs of battery replacements are also mentioned as very costly, there is, however, the potential to reduce these costs by using an energy harvesting solution.

Maintenance personnel is not in dangerous area: Many condition monitoring systems are certificated for hazardous environments. This means that maintenance personnel must operate in this environment to replace batteries. A low battery lifetime increases the number of necessary battery replacements and therefore also increases the risk for the workers. An autonomous self-powered CbM system would avoid battery replacements and therefore it would help to reduce the risk for maintenance personnel [44].

1.3 Goal of Thesis

In this thesis, an energy harvesting powered condition monitoring sensor node is developed in cooperation with *Analog Devices, Inc.* in form of a research project. A suitable method to monitor the condition of machines or gearboxes and sensors which meet the requirements have to be chosen. To power the system an energy harvesting solution has to be identified. To transmit the measured data to an analysis device a connectivity solution has to be used. The system needs to have low power consumption because of the limited energy harvested from the environment. The hardware and the firmware have to be designed to meet the low power requirements. The processing unit, sensors and the power management unit have to be energy-efficient and the firmware has to be designed to avoid long and power consuming active times of the devices. To use the available energy in an optimized way static intervals for transmitting data are replaced and a dynamic duty cycle is implemented to provide data as frequently as possible.

There are no CbM systems available which are powered by a Thermoelectric Generator (TEG) but shortly before finishing this thesis another work has been published which follows the same goal as this work: A CbM system which is powered by an energy harvester. The published work and another previous literature are described and their characteristics are discussed in 2.5. 2.6 points out the advantages of the sensor node developed in this work compared to systems described in these publications.

Figure 1.2 illustrates the goal of this thesis: A sensor node (blue box) is designed to acquire the condition of a machine and send the data to an analysis device for further processing, analysis, trending or archiving. The interpretation of the measured data, for example detection of a failure or a trend analysis of the remaining lifetime of the equipment, is not part of this work.
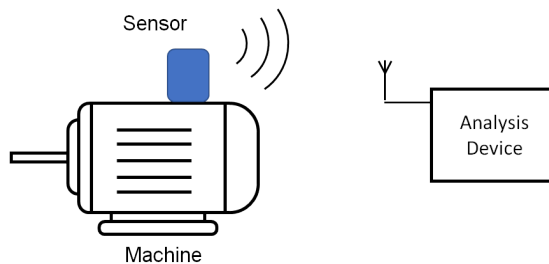

Figure 1.2: Illustration of a CbM system

2 State of the Art

This section describes the State of the Art for vibration-based condition monitoring and gives an overview about alternative methods for condition monitoring. Furthermore, available systems and standards for vibration-based condition monitoring are discussed. This section is completed with an analysis of previous works.

2.1 Vibration-based Condition Monitoring

Vibration analysis is the most common technique for monitoring the condition of a machien, often also called the health of a machine [COV+18] [ZFMW14] [GWWY18] [SK17]. Rotating parts always cause vibrations and therefore it is a widely used approach in the industry to analyse the condition of machines [MTPP12] [KV86] [HVD+15] [SK17] [KJLK10] [MAHH]. Accelerometers are commonly used sensors for vibration monitoring because they have a wide acceleration and frequency range. The possibility to measure high frequency is necessary for bearing and gearbox monitoring. Micro Electro Mechanical Systems (MEMS) accelerometers are widely used for condition monitoring because of the low cost, high reliability and low power consumption [SK17] [MV05].

Figure 2.1 shows an exemplary machines' health state as a function of operating time. Vibration monitoring can detect the decreasing health of equipment about 2 months earlier than the analysis of the noise would observe it [39] [29].

The development of MEMS technology enables MEMS accelerators being more popular for vibration-based condition monitoring.

In [HVD+15] mechanical faults on an electric motor are detected by vibration analysis using MEMS accelerometers. In this paper the ADXL203 dual-axis accelerometer from Analog Devices is used. It combines two sensor devices, amplifiers and a demodulator into one single integrated circuit (IC). Two different faults are analysed in this paper, misalignment of the shaft and loosening. Misalignment means that the axis of the motor shaft and the shaft of the load are not exactly coupled. There is an offset between the axis or an angular misalignment. Loosening is caused by a lack of structural stability. Many times the mechanical coupling of two shafts results in a combination of both failures. Spectral analysis allows to detect both faults, but it cannot differ between misalignment and loosening. Therefore, spectral and temporal analysis is used. [HVD+15] shows that loosening generates a clipped signal in the time domain. Frequencies
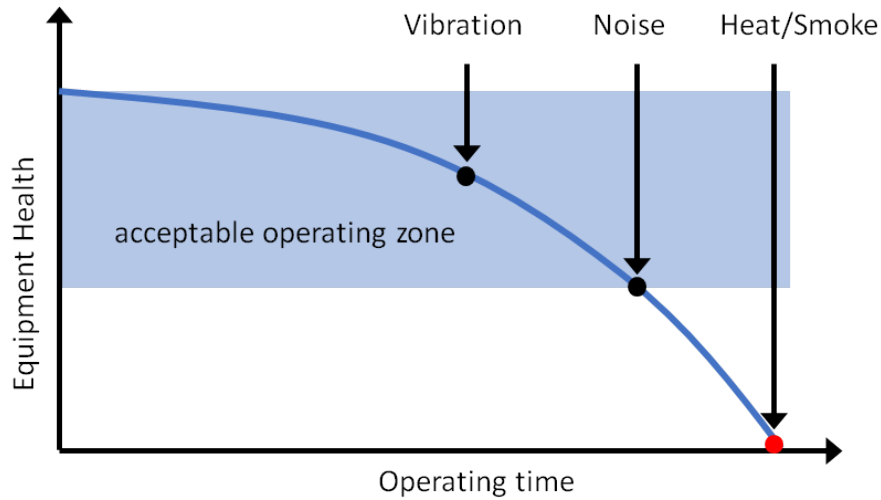
Figure 2.1: Decreasing machine health over time. Source: [39]

caused by loosening are two and four times the rotating speed. This is visible in the spectral analysis of the vibration signal.

Bearing fault or faulty rotor bars of induction motors are detected in [SK17] by analysis of the motor current and mechanical vibration. Mechanical stress caused by overload, abrupt load changes or electrical stress can lead to rotor bar breakage or bearing faults. The ADXL335 low power three axis accelerometer is used to monitor vibrations of the motor. Vibration data is sent to a computer and the spectrum is calculated by a fast Fourier transform (FFT) using MATLAB. The spectrum of the signal is compared to previously stored waveform of a healthy motor and a faulty motor can be detected.

In [MV05] vibration analysis is used to detect electrical faults in three-phase squirrel cage induction motors. Electric faults, e.g. unsymmetrical power-lines, causes electromagnetic forces which leads to vibration of the machine, various faults and their frequency characteristics are discussed. The ADXL202E accelerometer is used for vibration measurement. It is a low-cost dual axis accelerometer with duty cycle output. The vibration of a three-phase, 50 Hz, 5 HP induction motor is measured in six different cases (one healthy motor, five electrical faults). The monitored vibration data is sent to a FFT analyzer and the calculated FFT data is sent to a computer for visualization and documentation. The results of the vibration analysis are compared with the results of a Motor current signature analysis (MCSA):

- Using vibration analysis is more beneficial than MCSA as it may also detect mechanical faults in stator and rotor, e.q. rotor bar damage, end ring damage or air gap eccentricity.

- Electrical hazards can be avoided, as it is a non-electrical contact method.

- MEMS accelerometers are low cost, reliable, compact in size, light in weight, low power and combine a three-axis measurement device into one single IC chip which allows a cheaper and smaller condition monitoring system.

A wireless sensor node for monitoring the condition of induction motors is described in [KJLK10]. An on-line monitoring system including the small, low power, three-axis ADXL330 accelerometer

7

measures the vibration of a machine. For the experimental set-up the accelerometer is mounted on a three-phase, two-pole, 1 HP squirrel cage induction motor. The motor drives a flywheel, weights can be mounted on it to produce imbalance. To detect faults the Root Mean Square (RMS) value, the crest factor and the FFT of vibration data is calculated. The spectrum is compared with the spectrum of a healthy machine to detect faults. The RMS value increases according to the level of imbalance while the change of the crest factor is small, this means that the fault is not likely caused by a bearing. In the spectrum the frequency at ~50 Hz (rotating speed) has a dominant value depending on the level of imbalance. The used methods for fault detection worked satisfactorily for the given application.

A vibration-based energy harvesting sensor node for condition monitoring is presented in [ZFMW14]. A piezoelectric energy harvester is used to power a wireless communication system and a wide bandwidth accelerometer measures vibration. In subsection 3.1.2 the system is described in detail and the disadvantages are discussed.

In [GWWY18] accelerometers are used for healthy monitoring of railway tracks. The ADXL345 and the ADXL1001 MEMS accelerometers are used to measure vibration. The ADXL345 is an ultra low power three axis accelerometer and the ADXL1001 is a low noise, high frequency, single axis accelerometer. Furthermore, a temperature sensor, a humidity sensor and a human infrared sensor module are included in the monitoring system. For wireless data exchange a ZigBee network is used.

The following table shows some of the reasons for mechanical vibration and the frequencies at which they can be found [Gol99] [HVD+15]:

Table 2.1: Cause of likely frequencies in mechanical systems

Frequency	Cause	Comments
1/2 x rpm	Oil whirl	occur in sleeve bearings
1 x rpm	Unbalance, misalignment of couplings bowed shafts	The level is proportional with the grade of unbalance and has its maximum in radial direction
2 x rpm	Mechanical looseness, coupling unbalance	Loose bolts could be the reason for it
1 x, 2 x, 3 x, 4 x rpm	Misalignment of couplings, bearing and bent shaft	The level is greatest in axial direction
1 x, 2 x, 3 x, 4 x rpm of belts	Drive belt faults	Amplitude is pulsing
1 x, 2 x, 3 x frequency of electrical power	Electrical ground loops	Amplitude drops immediately after power is turned off
Number of blades x rpm and multiples of it	Faulty blades	High level could cause a stall
Blade frequency $\pm$ n x rpm/60 n = 1, 2, 3	Loose coupling	The level of the side bands is normally lower than the blade frequency
1 x rpm of gear Number gear teeth x rpm/60 x n n = 1, 2, 3, . . .	Eccentric pitch circle, tooth error in gear poor gear mesh	Poor mashing, wear of meshing surfaces, resonance of the gear train could be a reason. Harmonics could be due to skewed axes of rotation
Mesh frequency +- n x pinion rpm/60	Eccentric pinion, pinion shaft not parallel to bull gear shaft, poor pinion support	Higher amplitude of the side bands means a greater severity of the problem

Formula	Fault	Notes
Mesh frequency +- n x bull gear rpm/60	Eccentric bull gear, bull gear shaft not parallel to pinion shaft, bull gear shaft deflection	Higher amplitude of the side bands means a greater severity of the problem
$1/2\ Z\ f\ (1 + d/e\ \cos(\alpha))$	Spall, inner bearing race	f = rotational speed, Hz d = ball diameter, in e = pitch diameter, in α = contact angle, degrees Z = number of balls
$1/2\ Z\ f\ ((1 - d/e\ \cos(\alpha))$	Spall, outer bearing race	See above
$f\ e/d\ (1 - (d/e)^2\ \cos^2(\alpha))$	Spall, ball of bearing	See above
$1/2\ f\ (1 - (d/e)\cos(a))$	Cage umbalance	See above

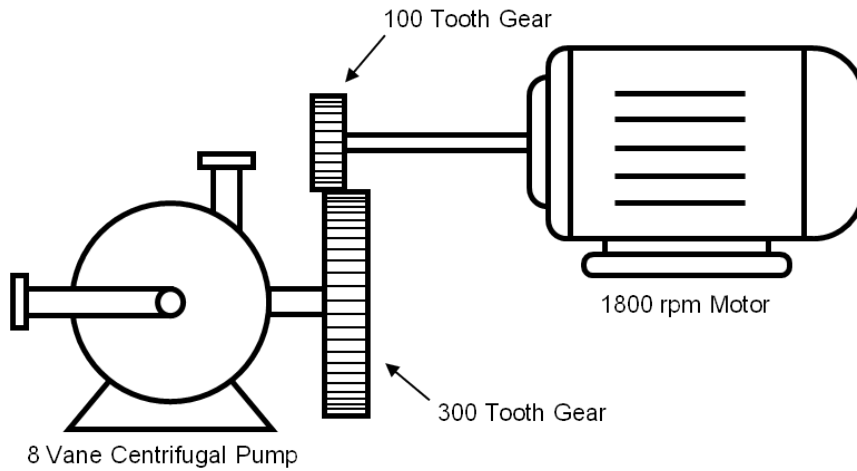**A typical mechanical system as an example**

Figure 2.2: A typical mechanical system. Source: [Gol99]

The following calculations show frequencies generated by the mechanical system shown in Figure 2.2. The frequencies can be measured in the whole system as the oscillations spread out via the material of the machine, only the amplitude will change when vibration is measured further away from the source. Other frequencies, such as side bands or multiples of the calculated frequencies can also exist. This example demonstrates that it is essential to be able to measure frequencies above $1\,kHz$ to detect bearing or gearbox faults.

$$\text{Motor shaft speed} = (1800/60)\,rpm = 30\,Hz$$
$$\text{Pump speed} = \frac{100}{300} \times 1800\,rpm = 600\,rpm \hat{=} 10\,Hz$$
$$\text{Gear mesh frequency} = 100\text{teeth} \times 1800\,rpm$$
$$= 300\text{teeth} \times 600\,rpm$$
$$= 180000\,rpm$$
$$\hat{=} 3\,kHz$$

The spectrum of the vibration generated by the mechanical system shows the expected peaks at the calculated frequencies [Gol99]. An increased level at $3\,kHz$ can indicate a faulty gear wheel, for example a damaged or broken tooth.

Frequency analysis of vibration is a widely used approach in CbM systems. The authors in [HVD+15] emphasize that machine faults can also be seen in time domain of vibration signals. For example loosening generates a clipped signal in the time domain. In this work the raw vibration data is transmitted to a computer where analysis in time and frequency domain can be done.

2.2   Systems for Vibration-based Condition Monitoring

There are many machine monitoring systems for different applications available. Some of them are big and need an external power supply which limits the field of application [Gol99] [27] [AAB16]. Another disadvantage is the fact that external sensors are connected via a cable to the monitoring device which is an additional source of errors, for example broken cables or loose connectors.

The following section describes battery powered CbM systems and their advantages and disadvantages are discussed:

ONEPROD EAGLE [22] is a wireless system for condition monitoring. It is a small battery powered device which measures the vibration and also the temperature and sends it to the wireless gateway. A Lithium thionyl chloride (Li-SOCl2) D-size cell is used as an energy source. The battery is non-rechargeable and a costly battery replacement needs to be done once its lifetime has been reached. If sending the on-board calculated spectrum and the time waveform once a day, the battery lasts up to 5 years but this can be less when using it at deviant environmental conditions. Transmitting data once a day is sufficient for condition monitoring but the limited battery lifetime is a disadvantage of this system. If critical machine measurements are performed more often then battery-lifetimes decreases to two years, this leads to higher battery and maintenance costs. The range of the wireless communication can be extended up to a hundred meters with the help of wireless expanders, this allows monitored machines to be further away from the gateway. The sensor and the expander are certified for explosive area zone 0 (North American classification: Class I Division 1) usage, this means that it can be used in a permanent or long term explosive gas environment [3]. They are also IP67 certified, which means they are dust-proof and immersion for less than 30 minutes at a depth of less than one meter will cause no harmful damage [11]. Zone 0 and IP67 certification allows a wide range of operating environment. The tri-axial piezoelectric sensor measures vibration from $1\,Hz$ to $15\,kHz$ for the Z axis and up to $6\,kHz$ for the X and Y axis of accelerations up to $\pm50\,g$. The frequency and the acceleration range are suitable for CbM systems but there is no available information about the sensitivity of the sensor. This condition monitoring system allows post-processing and analysis of the vibration data in time and frequency domain with the goal to detect all possible faults of a machine. The combination of time and frequency analysis increases the chance of detecting a machine fault.

The SmartDiagnostics Vibration Sensor Node (SD-VSN-02) [19] from KCF Technologies is a sensor node for machine condition monitoring. The sensor is part of a whole predictive maintenance system for pumps, motors and other rotating machines. The system is IP65 certified which means that it is dust-proof and water jets lead to no harmful effects [11]. There is also a SD-VSN-2N model which is suitable for hazardous conditions. It is certified for ATEX zone 2 (North American classification: Class I Division 2). The integrated accelerometer measures vibrations up to $\pm19\,g$ at frequencies up to $4\,kHz$. This acceleration limit might be too low for some machines. To detect high frequency faults the frequency range of this system is also too low. The sensor node is powered by a $3\,V$ Lithium Manganese Dioxide (LiMnO2) (CR123A) battery, an available guide describes how an operator can replace the battery in the field. This saves the high costs of a battery replacement by the manufacturer. The lifetime of the battery can be up to eight years when data is sent once an hour and gets lowered to two years when data is sent every 2,5 minutes. If it would be possible to use a higher data update interval, the battery lifetime could be higher but transmitting intervals can only be set between 2,5 and 60 minutes. The vibration data is measured and the spectrum is calculated locally before it is sent to the

receiver. If only the spectrum is analysed some machine faults can stay undetected and therefore the reliability of the system is not as high as it would be with analysis in time and frequency domain.

The AV Sensor 2000R [4] from AMC VIBRO is a sensor unit for continuous monitoring and machine diagnostic. The sensor is dust-proof and protected against water ingress for less than 30 minutes and less than one meter deep (IP67). This offers a wide range of operating, but it cannot be used in hazardous environment. If there is a communication problem, data is stored in an internal memory and is sent as soon as there is a re-connection with the effect of no missing data. The two vibration channels can measure vibration up to $\pm 20\,g$. The frequency range of the accelerometers is up to $10\,kHz$ and the sensitivity is $100\,mV/g$. The frequency range and the sensitivity are good for CbM systems, but the acceleration range limits the area of operating. The sensor node is powered by two AA $3,6\,V$ Li-SOCl2 batteries which have a limited lifetime of six years when a one-second measurement is done every eight hours, this measurement interval cannot be changed to increase the battery lifetime. The battery used to power the sensor is non-rechargeable and has to be replaced at the end of its lifetime which is time-consuming and costly for the user. The vibration acceleration is measured and several statistic parameters are calculated [40]. There is no access to the raw vibration data for calculating the spectrum and no analysis in the frequency domain is done. Some machine faults could stay undetected and therefore a combination of time and frequency analysis should be used for a reliable CbM system.

The SKF Machine Condition Indicator [Inc13] is a vibration sensor for monitoring non-critical machines especially with constant operating conditions. This device has no interface to transfer measured data. There are just three light-emitting diodes (LEDs) which shows the condition of the machine. There is no access to the measured vibration data which makes this system unsuitable for condition monitoring. A non-replaceable, $3,6\,V$ lithium battery is used to power this sensor which makes these devices more cost-intensive and wasteful because the whole sensor needs to be replaced instead of only replacing the battery. Internal sensors measure velocity from $10\,Hz$ to $1\,kHz$ and the surface temperature of the machine from $-20\,°C$ to $105\,°C$. The low frequency range of the machine condition indicator and the fact that there are only visual alarm indicators makes the sensor unsuitable for machine condition monitoring.

The CMWA 8800 [16] is a wireless machine condition sensor and combines a sensor, data collector and radio into one device. The vibration data is sent in bursting or polling mode, bursting mode means that the data is sent in programmed intervals while in polling mode the transmitting is triggered over the radio, this option offers a customized operation. These sensors can also be programmed as router nodes which allows them to forward data from other sensors with the effect of a higher network range. The device is certificated for ATEX zone 0 and protected against solid objects and liquid with class IP66, this offers a wide range of operating environments. The internal sensor is only a single axis sensor and measures velocity in a range from $10\,Hz$ up to $1\,kHz$. The frequency range can be too low to detect some machine faults and vibration is only measured in one axis. The device is powered by an internal $3,6V$ Li-SOCl2 cell that has a battery lifetime of up to five years, high or cold temperatures decreases the battery lifetime to three years. The battery cannot be recharged and has to be replaced by SKF, which makes the battery replacement process costly because maintenance personnel from the producer have to be requested to replace the battery or the machine condition sensor needs to be sent to the manufacturer. The low frequency range and the battery replace process are disadvantages of this system. Velocity and acceleration are measured by the sensor and the spectrum is calculated by the analysis software. The combi-

nation of analysis in time and frequency domain increases the chance of detecting a machine fault.

The VTS211 wireless vibration and temperature sensor [SW17] from Sensor-Works is a battery powered sensor for condition monitoring. The internal piezoelectric accelerometer measures the vibration data in a range of up to $\pm 20\,g$ and up to $10\,kHz$. The wide frequency range offers a wide range of application but the acceleration range limits the area of operation. A temperature sensor measures the temperature in a range from $-30\,°C$ to $85\,°C$. The casing of this device is IP66 certificated and ATEX II IG certification is pending, therefore a wide area of application is available. The sensor uses the latest Bluetooth low power standard for communication and it can be used as a standalone device or in a network consisting of many sensors. The configuration and firmware upgrade can be done over the radio network. This allows an easy adaption of the configuration. This sensor doesn't calculate the spectrum or other characteristics of the vibration data. After a vibration measurement is done the raw vibration data can be sent to an analysis device. This approach enables a battery life of up to five years on default measurement interval, which is not defined in the data sheet. The $3,6\,V$ Li-SOCl2 battery is not rechargeable but can be replaced in the field. The fact that the battery can be replaced at the location where the sensor is placed saves time and personnel costs for the replacement itself but increases costs for new batteries and also increases waste.

The biggest disadvantage of the condition monitoring systems listed above is the fact that they are battery powered. Every battery has a limited battery lifetime and needs to be changed eventually. If there are many machine health monitoring devices, it means that there are many batteries which need to get changed when they are empty. This can be very time-consuming and expensive for the company and there are further losses if machines need to be shut down for the battery change.

TELEMAQ [TEL] developed battery-less modules with internal sensors powered by energy harvesters. Two evaluation kits are available: The M-400-G-BLE and M-2000-G-BLE, both modules are powered by a vibration energy harvester with internal accelerometers. The energy harvester is designed to convert mechanical vibrating energy into electrical energy by piezoelectric coupling. The best energy density is at a frequency range from $50\,Hz$ to $300\,Hz$ while the acceleration is between $0.2\,g$ and $1\,g$. The output power of the energy harvester is $400\,\mu W$ for the M-400-G-BLE and $2000\,\mu W$ for the M-2000-G-BLE. There are also modules with $700\,\mu W$, $1000\,\mu W$ and $1500\,\mu W$ available. The energy harvesting solution powers the internal sensors and external sensors can be connected to the device and powered through the energy harvester. Integrated sensors can be temperature sensors, accelerometers, magnetometers and others. Both evaluation kits measure vibration data in a range from 20-300 Hz, but there is no further information about the sensor available.

A disadvantage of this vibratory energy harvesting modules is the fact that the vibration characterization must be done before using the devices. For an optimal efficiency of the energy harvester it must be tuned corresponding to the vibration source. This makes it unsuitable for changing machine operating conditions. Another disadvantage is the frequency limit of the energy harvester, this makes it unsuitable for low-speed or high-speed rotating machines. The possibility to connect different external sensors make it applicable for a wide range of applications.

2.3   Other Condition Monitoring Methods

This section gives a short overview of different condition-based monitoring methods.

Electric effect monitoring
:   Condition monitoring for motors or generators is often done by monitoring the voltage and
the current of the equipment [MTPP12] [SK17]. Unusual phenomena in voltage and current
can be analysed and failures can be detected. To be able to measure the voltage and the
current the monitored machine might need some changes or modifications. The installation
of such a system is time and cost consuming as the machine might need to be shut down
during installation. The modifications which needs to be done to monitor the voltage and
the current might vary from machine to machine. In this work a different method is chosen
to allow an easy installation of the system even after the machine is already in operation.

Oil analysis
:   Every moving part in motors, generators or gearboxes need to be lubricated with oil or
another lubricant. Small pieces such as splinters caused by damaged equipment can be
used to indicate failures before they end up in the oil filter. A sensor can detect solid
objects in the oil, if there are more or bigger pieces in the lubricant it can indicate a broken
part of the machine [MTPP12]. This method is unsuitable for an installation afterwards
as the machine need to be changed or modified for this method. Therefore, in this work a
different approach is chosen to monitor the condition of a machine.

Temperature monitoring
:   Temperature sensors can be used to monitor the temperature of electric equipment. The
housing temperature of a machine can be influenced by many things; the external environ-
ment, the load of the machine or because of a failure. Therefore, it is important to know
if a change of temperature is caused by a fault, a higher load or just because of chang-
ing environment conditions. Temperature monitoring reacts slowly because temperature
changes in the machine happens slowly, therefore it is possible that a failure is detected too
late [MTPP12]. This method is not as efficient for early fault detection compared to other
methods and therefore it is not chosen in this work [39] [29].

Acoustic emission
:   The acoustic emission (AE) method is similar to vibration measurement. Due to dynamic
deformation processes within a material energy is released in the form of waves [TWO$^+$14].
Acoustic emission testing is known as a non-destructive testing method for products [14].
AE sensors measure the vibration in a range from $50\,\mathrm{kHz}$ up to $1\,\mathrm{MHz}$ [TWO$^+$14] [1] [15] [2].
Only a few machine faults occur in this frequency range and therefore some machine faults
might not be detected. Other disadvantages of this method are the high costs [TWO$^+$14]
and that the sensor must be located close to the source because of the attenuation of the
signal and this can limit the range of application [MR06].

2.4   ISO Standards

The ISO 20816-1 "Mechanical vibration – Measurement and evaluation of machine vibration –
Part 1 General guidelines" [iso16] is an instruction for measuring and rating the vibration of a

machine. ISO 10816 "Mechanical Vibration - Evaluation of machine vibration by measurements on non-rotating parts" is for measurements on non-rotating parts of a machine, for example bearing housings. For some machines it can be necessary to do additional measurements on rotating parts, for example on shafts. In this case the ISO 7919 "Mechanical vibration - Evaluation of machine vibration by measurements on rotating shafts" must be applied.

The vibration measurements can be done for tests, inspections or to monitor the operating condition of the machine. For different types of machines there are separate parts of the standards available which defines the parameters for the vibration measurement. The standards define operating zones for the machines based on amplitude, velocity and acceleration of the vibration. They also give information on how to set thresholds, - alarm and shut-down - to give a warning or to shut-down the machine in case of a failure. A low amplitude of vibration acceleration means zone A and identifies a safe operating condition. Figure 2.3 shows a typical chart of the zones as a function of the frequency.

Zone A: Vibrations of new machines are usually in this area [iso16].

Zone B: Machines with vibrations in this zone are normally in good condition and convenient for continuous operation. Effort to reach zone A might be out of scale and unnecessary and therefore vibrations in zone B are acceptable [iso16].

Zone C: Machines with vibrations in this zone are usually unsuitable for continuous operation. The machine can be in operation for a limited time until there is a convenient opportunity for maintenance [iso16].

Zone D: Vibrations in this zone are dangerous and can cause damage to the machine, the machine should be shut down [iso16].
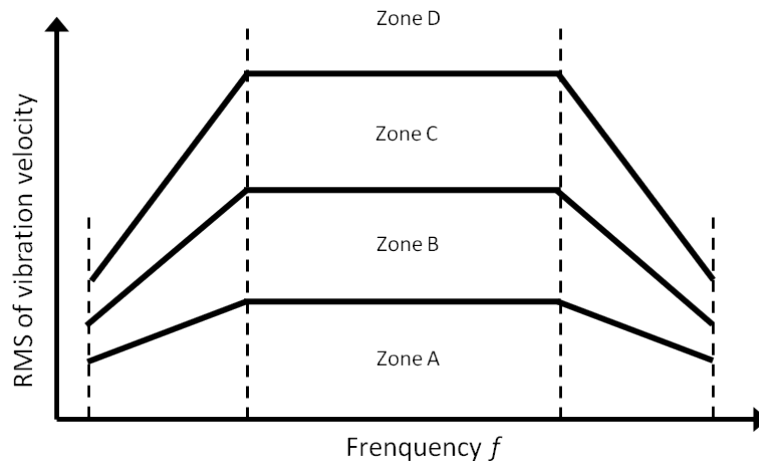

Figure 2.3: Typical zone limits as a function of frequency. Source: [iso16]

The limits of the zones depend on the type, the size and the mounting of the machine. Figure 2.4 shows typical RMS values of the velocity of the vibration for medium-sized and large machines with different mounting [iso17]:

ISO 10816-3	Medium-sized machines		Large machines	
Velocity	Rated Power			
mm/sec RMS	15kW - 300kW		>300kW	
11,00				
7,10				
4,50				
3,50				
2,80				
2,30				
1,40				
0,07				
0,00	Rigid	Flexible	Rigid	Flexible
	Foundation			

Figure 2.4: Typical zone limits as a function of vibration velocity: [iso17]

The values defined in the standards are not specified for acceptance test. The values are more likely a reference to know if the values defined by the machine producer and controller are realistic and achievable. Special machines might require specific values. The reasons for these specific values must be explained and it has to be confirmed that the machine can operate without risk under this specific conditions [iso17].

2.5 Previous Work

TEGs are often used to harvest energy from a human body for wearable devices [TSM+17] [31] [37] [35]. This section discusses two previous works which use thermoelectric energy harvesters to power condition monitoring systems for mechanical systems:

In [WBV+11] an energy-autonomous sensor is developed for condition monitoring on a rotating shaft. A prototype of a TEG is built to power the wireless CbM system. Sensors and TEGs are separated and both are mounted on the shaft. The TEG is connected with the sensor via a cable and provides the needed electric energy for it. The sensor monitors the vibration of the shaft and sends the data wirelessly to an analyse computer, a wired sensor is used as a reference. The TEG is mounted on the shaft close to the gearbox where the highest temperature increase happens. To avoid shaft imbalance due to the TEG a proper weight balancing needs to be done during the TEG design. See Figure 2.5 for the architecture of the system presented in [WBV+11].

The sensor used in this system has a measurement range of ± 16 g which limits the rotating speed of the machine. The maximum centripetal force which can be measured is 15 g plus 1 g earth gravity (=16 g), this limits the rotating speed to 692 rpm before the sensor's Z-axis is in saturation. Using a sensor with a higher measurement range would increase the maximum rotating speed of the machine. Another disadvantage is that a cable is needed to connect the TEG
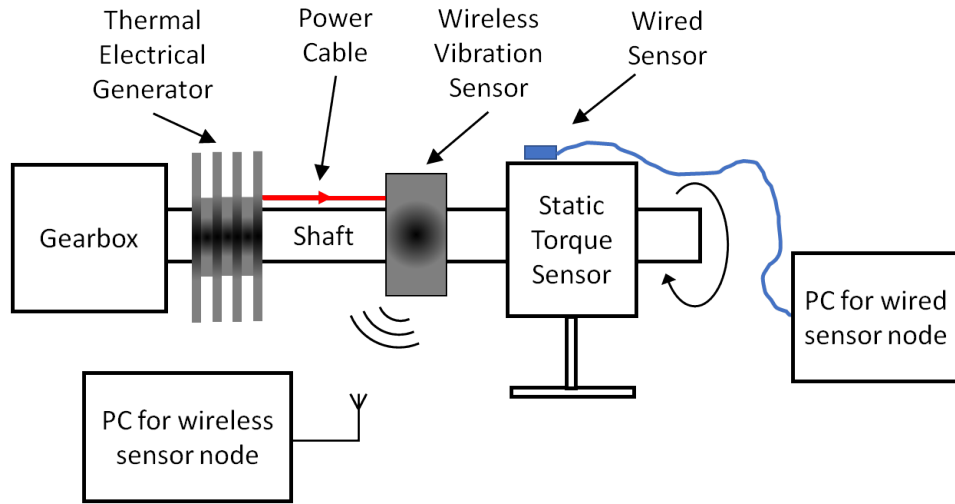
Figure 2.5: System architectur of CbM system. Source: [WBV+11]

with the wireless sensor which adds additional sources of errors, for example a loose connector, and the fact that the system is separated into two devices increases the dimensions of the whole system, also the machine needs to be stopped to mount the TEG and the sensor on the shaft. The experiments in this paper show that the TEG produces enough energy so that data can be continuously sampled at a sampling rate of 1600 samples per second (SPS) and transmitted to an analyse computer. When data is transmitted periodically the size of the TEG could be smaller with less output power because continuous data transmitting is not necessary for a CbM system. Measurements once a day is a good compromise between permanent and intermittent monitoring [Ran11]. A case study in [8] confirms this statement as it shows that 10 weeks are between the detection of a higher vibration level and the failure of the machine.

In [COV+18] a TEG based, self-powered machine condition monitoring sensor node is presented. A thermoelectric energy harvester is used to convert the waste heat from a machine the system is mounted on, into electric energy to power the sensor node. As test set-up a retrofitted speaker is used as heat and vibration source. The heart of the design is the ADuCM3029 Microcontroller Unit (MCU) which manages the tasks and transmits the data via a radio module to a phone, see Figure 2.6. The ADP5092 Power Management Unit (PMU) is designed for ultra low power applications and converts the low voltage from the TEG into higher voltage and stores the energy in the storage element. The whole system is small and all sensors, the MCU, the radio module, the PMU, the TEG and the super cap are together on one printed circuit board (PCB). The system consists of four sensors:

- ADXL362: The micropower, three axis accelerometer is used to wake up the microcontroller when a vibration threshold is reached or after a fixed time interval. The approach to wake up the MCU when a vibration limit is exceeded is unsuitable for a CbM system because a low vibration level in various frequencies can also indicate a failure. Some harmonics can have high amplitude in good machine condition while others might be low and only slightly increase when a failure arises. To wake up the MCU periodically the internal timer or RTC can be used.

- ADXL355 and ADXL372: A combination of both sensors is chosen to cover a wide dynamic

range of 25 μg to 200 g. The ADXL355 is a good choice because of the high sensitivity from 3,9 μg/LSB to 15,6 μg/LSB respectively to the measurement range. The bandwidth of the ADXL372 is 3200 Hz and this is too low for a reliable CbM system. Gearbox or bearing frequencies above 3200 Hz might indicate a failure and therefore a sensor with a higher frequency range should be used.

- ADT7302: This additional temperature sensor is not required because the ADXL355 accelerometer has an integrated temperature sensor.
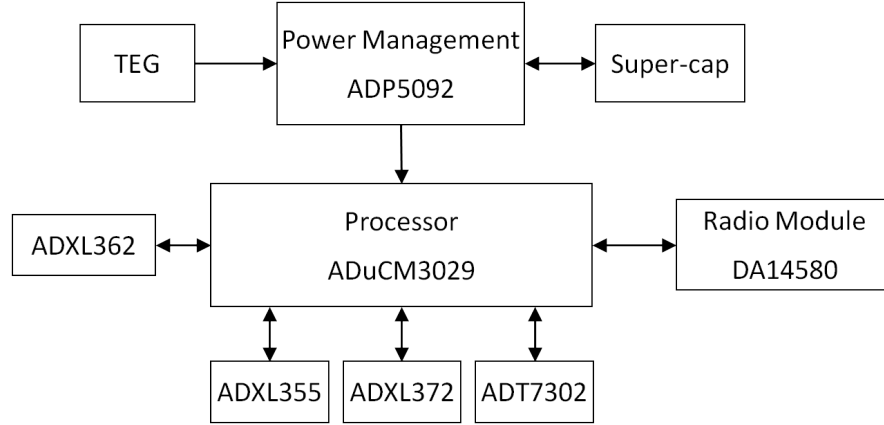
```
┌─────────┐      ┌──────────────────┐      ┌─────────────┐
│   TEG   │─────▶│ Power Management  │◀────▶│  Super-cap  │
└─────────┘      │     ADP5092       │      └─────────────┘
                 └──────────────────┘
                          │
                          ▼
┌─────────┐      ┌──────────────────┐      ┌─────────────┐
│ ADXL362 │◀────▶│    Processor      │◀────▶│ Radio Module│
└─────────┘      │    ADuCM3029      │      │   DA14580   │
                 └──────────────────┘      └─────────────┘
                    │      │      │
                    ▼      ▼      ▼
              ┌───────┐┌───────┐┌───────┐
              │ADXL355││ADXL372││ADT7302│
              └───────┘└───────┘└───────┘
```

Figure 2.6: Block Diagram of the system. Source: [COV$^+$18]

After the vibration measurement a FFT is performed to calculate the spectrum of the vibration data and the 50 largest coefficients are transmitted to the phone. Pre-processing can decrease the amount of data which needs to be sent but on the other hand it consumes energy on the sensor node. Reducing the 1024 samples vibration data to 50 coefficients leads to information loss and a machine fault could stay undetected. Therefore, it would increase the reliability of the CbM system when all vibration data is sent for further processing and analysis.

The power consumption for this system is only 12 μW when data is sent every 30 minutes and 200 μW for a data update rate of 30 seconds. A very low temperature difference on the TEG of 2,4-10 °C is sufficient to cover this operating range.

2.6 Advantages of this Work in Comparison to the Literature

The frequency range of the sensors in [COV$^+$18] limits the area of application and therefore, this sensor node is unsuitable as a reliable CbM system. The ADXL1002 sensor used in this work has a higher frequency range which covers a wide range of frequencies where possible failures can happen. The reduction of the raw vibration data to 50 FFT coefficients leads to an information loss. Only less than 10 % of the available information is transmitted for further processing or analysis which is another disadvantage of this sensor node. The data transmitted by the sensor node includes the raw vibration data in a high frequency range for X, Y and Z axis. Using an accelerometer to trigger a measurement process when a specific vibration level is reached is unsuitable because also a low vibration level in various frequencies can indicate a failure. Another option to trigger a measurement are pre-defined intervals which don't use the harvested energy in an optimized way. If the stored energy in the super cap is too low for a measurement and

transmitting process, the output voltage of the PMU will be disabled and the MCU and sensors are shut down. On the other hand, the sensor node will stay in sleep mode until the next measurement interval while already enough energy could be stored in the super cap. To avoid these drawbacks a dynamic duty cycle is implemented to check the voltage level at the super cap and to get the knowledge if enough energy is stored to perform a measurement and data transmitting process. In [COV+18] all sensors are sent to sleep mode after data is acquired. This means that the sensors still consume energy even when they are idle. The solution for this drawback is that the sensors are powered by the MCU or can be disabled by the MCU. This has the effect that the sensors are unpowered and don't consume energy when they are idle.

The TEG and the sensor used in [WBV+11] is mounted on the shaft which limits the rotating speed of the machine and it is also limited to detect failures only on the shaft. The devices have to fit the shaft of the particular machine which makes this system unsuitable for general applications. The sensor node developed in this work can be placed in a small case and mounted on every non-rotating parts of a machine. As the vibrations caused by the shaft can also be detected on bearing houses the developed sensor node is able to detect these failures as well.

3 System Design Approach

This chapter describes the different parts of the design, why they are chosen and what their tasks are. First, the energy harvester and the PMU are defined, followed by the sensors, the control unit and the radio solution. Then the design of the system is described, and a power consumption estimation is illustrated. The following figure shows the principle design of the condition monitoring sensor node: The energy harvester converts the energy from the environment into electrical energy. The PMU regulates the incoming energy, stores it in the storage element and provides electrical energy to the system. The microcontroller and the sensors measure the vibration and send the data via Bluetooth to a phone or a computer for further processing, analysis, trending and archiving.
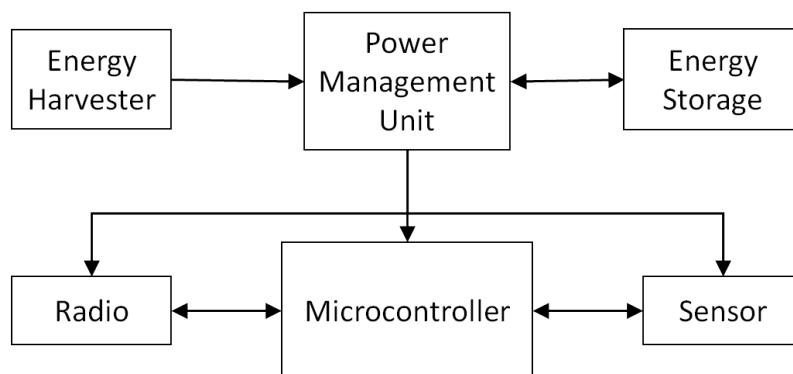

Figure 3.1: Block design showing the concept of this work

3.1 Energy Harvesting

For powering the sensor node an energy harvesting solution is needed. Energy harvesters use the energy of their surroundings to generate electric energy. Energy harvesting is well-known from windmills, water power plants and solar power systems on the roof of buildings, so-called macro energy harvesters. Micro energy harvesters are becoming more popular now and researchers focus on these systems which can generate up to a few hundred milliwatts from their environment [MR10].
See Table 3.1 for a comparison of energy source, solutions and the goal of macro and micro energy harvesters [MR10].

Table 3.1: A comparison of macro and micro energy harvesters. Source [MR10]

	Energy source	Solutions	Goal
Macro	Renewable energy (e.g., solar, wind water)	Energy management solutions	Reduce oil dependency
Micro	Energy from the environment (e.g., vibrations, heat, movement)	Ultra-low-power solutions	Perpetual devices

Popular sources for micro-energy harvesting are [21]:

- Mechanical energy from vibration, mechanical stress or strain

- Thermal energy in the form of waste heat from engines, generators, heaters or other machines

- Light energy from sunlight or indoor light

- Electromagnetic energy from electromagnetic waves

- A combination of mechanical and thermal energy generated by the human body

Energy harvesting can be used in medical sector to replace batteries in pacemaker [33] [28] or other implants, to power fitness tracker, make IoT systems battery-less and many other applications. A comparison of different energy harvesting methods shows that the following methods are most suitable to power a CbM system [CC08]: Solar, vibration and thermal energy harvesters. Table 3.2 shows an estimation of how much energy can be harvested from different ambient energy sources. Due to the fact that the harvested energy depends on many factors, for example, displacement and frequency of the vibration, brightness of the light and temperature difference, the values in the tables variegate.

The following list points out the benefits of energy harvesting solutions [EnO15]:

- Lower planning and installation costs because of the absent wires.

- The place of the sensor is flexible because it is self-powered.

- As there are no battery replacements required it is maintenance free for more than 20 years.

- A self-powered device has the same functionality as a wired device.

- The energy harvesting solution is reliable.

- As there are no battery replacements there is no hazardous waste disposal.

Table 3.2: Energy Harvesting sources

Energy Source	Typical Power Density / Power Output		
	source: [MR10]	source: [BO15]	source: [TP10]
Vibration/Motion			
Human	$4\,\mu W/cm^2$	$1\,\mu W$ - $20\,mW$	$4\,\mu W/cm^3$
Industry	$100\,\mu W/cm^2$		$800\,\mu W/cm^3$
Temperature Difference			
Human	$25\,\mu W/cm^2$	$0{,}5\,mW$ - $10\,mW$	$60\,\mu W/cm^2$
Industry	1-$10\,mW/cm^2$		$135\,\mu W/cm^2$
Light			
Indoor	$10\,\mu W/cm^2$	$<500\,\mu W$	$100\,\mu W/cm^3$
Outdoor	$10\,mW/cm^2$	$0{,}15\,mW$ - $15\,mW$	$100\,mW/cm^3$

Energy Source	source: [24]	source: [DS08]
Vibration/Motion		
Human	$1\,\mu W$ - $20\,mW$	100 - $400\,\mu W/cm^3$
Industry		
Temperature Difference		
Human	$0{,}5\,mW$ - $10\,mW$	$<100\,\mu W/cm^3$
Industry		
Light		
Indoor	$<500\,\mu W$	15 - $15000\,\mu W/cm^3$
Outdoor	$0{,}15\,mW$ - $15\,mW$	

3.1.1 Solar Energy

Photovoltaic cells are available in many different sizes and characteristics. Solar modules generate direct current (DC) which is proportional to the incident light. The fact that energy can only be harvested when light is available limits the application area in terms of place and time. During the night there is no sunlight available and no energy can be harvested. If the sensor node is placed at a location where no or limited sunlight is available, this energy harvesting solution is less efficient. Condition monitoring systems are often mounted in rough environments, the solar energy harvester can get dirty with oil or dust and this would decrease the efficiency of the energy harvester. To avoid these limitations, solar energy harvesting is not used to power the sensor node developed in this work.

3.1.2 Vibration Energy

While monitoring the vibration of a machine it seems to be the most likely approach to power the sensor node with a vibration energy harvester. A vibration energy harvester converts kinematic energy into electrical energy. The output power of such devices depends on the frequency and the acceleration amplitude of the vibration. This effect can be seen in Figure 3.2 which shows the output power of a vibration energy harvester as a function of the vibration frequency for

different acceleration amplitudes [CAP08]. If the frequency of the vibration is not in the range of the resonance frequency of the device, the efficiency of the vibration energy harvesters is lowered. The frequency and amplitude dependency is a disadvantage of this type of energy harvester. Nowadays machines are operated at a higher rotating speed and with higher loads in more flexible operating conditions, for example, full load and partial load [iso16]. Changing rotating speed of motors or generators, changes the vibration characteristics and that also changes the efficiency of the harvester [WBV+11] [PPA17] [ZFMW14]. The efficiency of the energy harvester is only high when the vibration has a steady vibration (for example no random shocks) and a dominant frequency. Some vibration energy harvesters allow adjusting the resonant frequency of the device by adjusting the clamp position and/or the tip mass [PPA17]. This allows adapting the energy harvester to the vibration of the given machine but the lower efficiency at changing operating conditions remains.

Vibration Energy Harvesters from Perpetuum Ltd [Ltd13] have a high output power of up to 27,5 mW and can be used as an external power supply to power wireless sensor nodes. The dimensions of the device are comparable to the CbM system described in section 2.2. The energy harvester is a cylinder with a diameter of 70 mm and a hight of 65 mm. The big dimensions and the fact that an external sensor node needs to be connected via a cable makes it inconvenient for a small and compact CbM system. Figure 3.2 shows the output power of the PMG17 Micro-generator from Perpetuum. It can be seen that the output power has a high dependence on the frequency and the acceleration of the vibration.
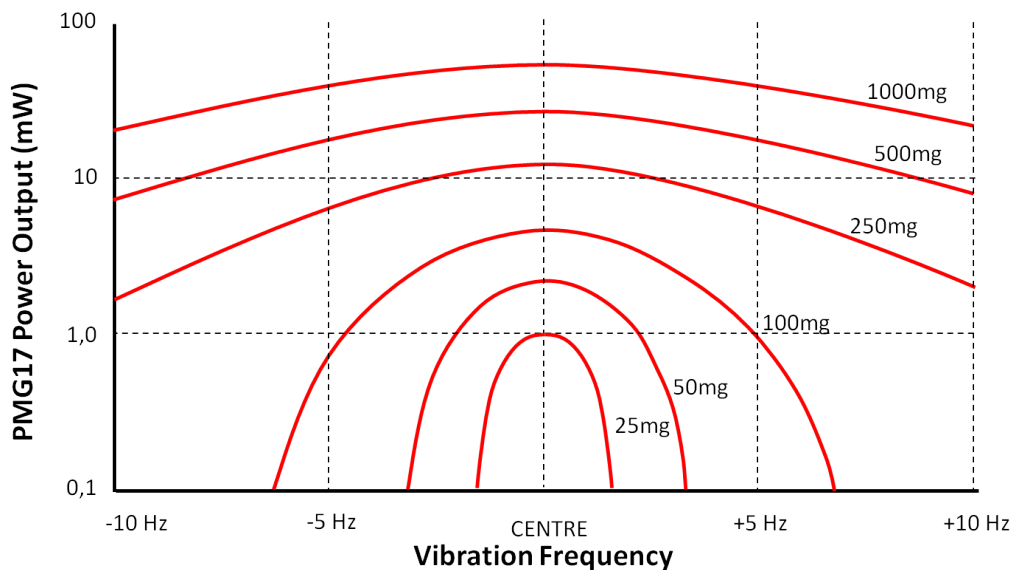

Figure 3.2: PMG17 output power as function of vibration frequency and vibration acceleration. Source: [CAP08]

In [ZFMW14] a wireless sensor node for mechanical vibration monitoring is presented. The self-powered sensor node uses a vibration-based energy harvester as an energy source. The MSP430F2013 ultra-low power microcontroller is the heart of the sensor node. It samples data from the ADXL001 accelerometer and sends it via the CC2520 wireless module to the receiver. Some problems stayed unsolved in this paper. One problem with the energy harvester is that it should be designed respectively to the vibration source. Adapting the energy harvester to the specific vibration source makes it inefficient for changing operating conditions because the

vibration changes with the rotating speed of a machine. Another problem is that the duty cycle needs to be set so that the power consumption of the system is equal or less than the energy produced by the energy harvester. While the system is in sleep mode the energy harvester needs to harvest enough energy to power the system for the next measurement task. Changing operating conditions make it hard to estimate the energy harvested by the energy harvester and therefore an accurate duty cycle cannot be pre-calculated.

The first problem can be solved by using a different energy harvester solution, see section 3.1.3. To handle the second problem a solution can be implemented where the voltage at the storage element is measured. The knowledge of the voltage gives information about how much energy is stored and if there is enough energy to perform a vibration measurement. This would avoid pre-set duty cycles and would make the system more flexible in terms of measurement intervals and providing data.

3.1.3 Thermal Energy

The condition monitoring sensor node in this work is designed with a TEG as an energy source because of the disadvantages of vibration energy harvesters and solar energy harvesters. The dimensions of TEGs can be very small which allows small system dimensions. The output power of such a device depends on the temperature difference across it. TEG characteristics, e.g. output voltage and output power, have to fit the power management unit described in the next section but there are no limits in terms of manufacturer. The TEG used in this work is the EHA-PA1AN1-R04.

How Thermoelectric Generators work: The Seebeck Effect
The Peltier effect and Peltier elements are known for their refrigeration applications: In picnic baskets or cool boxes, Peltier elements are used to keep food or drinks cold. Another application of these devices is the use as cooling for laser diodes or other electronic devices. The Seebeck effect can be seen as the inverse Peltier effect and is used by TEGs to convert heat energy into electric energy. A temperature difference between both sides of a TEG generates an output voltage which is proportional to the temperature difference [9] [10]. Figure 3.3 shows the principle of such a device.
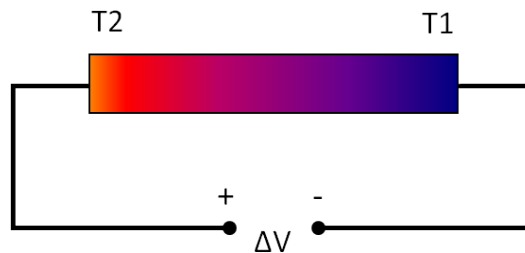

Figure 3.3: Seebeck effect. Source: [43]

Knowing the temperatures (T1, T2) and the Seebeck coefficient (S) of the material allows the calculation of the generated voltage ΔV, see the formula below. For p-type materials the Seebeck coefficient is positive, for n-type materials it is negative [43].

$$\Delta V = -S \times (T_2 - T_1)$$

Two dissimilar metals, p-type and n-type, are necessary for TEGs. The two metals are electrically connected on one side and a temperature difference has to be applied across the two surfaces of the TEG, see Figure 3.4.
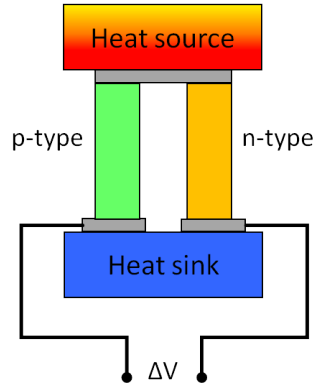

Figure 3.4: Schematic diagram of a TEG. Source: [43]

Recent development in TEG technology focuses on chip-scale TEGs which have a smaller device area compared with traditional bulk TEGs and this allows smaller system dimensions. The optimized manufacturing process also decreases the costs and increases the output voltage of the devices [43].

Energy Harvester used in this Work: EHA-PA1AN1-R04
The EHA-PA1AN1-R04 is a mini energy harvester produced by Marlow Industries. It is a low cost, small package thermal energy harvester which is designed for "solid to air" applications with a cooler mounted on the package, see Figure 3.5. The design of the cooler makes it suitable for vertical and horizontal surfaces. The maximum acceptable temperature on the hot side is 85 °C; a higher temperature might destroy the device. Table 3.3 shows the characteristics of the device depending on the temperature difference across the TEG [18].

Table 3.3: EHA-PA1AN1-R04 characteristics

Air Flow (MPH)	0	3	0	3
Hot Side Temperature (°C)	85	85	55	55
Cold Side Temperature (°C)	25	25	25	25
Gross Power (W)	0,005	0,035	0,001	0,01
Open Circuit Voltage (V)	0,27	0,8	0,11	0,4
Matched Load Voltage (V)	0,11	0,39	0,06	0,02

Other manufacturers, such as, Ferrotec, Kryotherm, Laird Technologies and TE Technology produce thermoelectric modules in different sizes with different characteristics which can be used to power a self-powered sensor node.

Figure 3.5: EHA-PA1AN1-R04 Energy Harvester

3.2 Power Management Unit and Energy Storage

The ADP5092 is an ultra-low power energy harvester PMU for self-powered wireless sensor devices, portable and wearable devices and other low power applications [Dev17b]. The harvested energy from photovoltaic cells or TEGs is used to charge reachable Li-Ion batteries, thin film batteries or super capacitors and to power the system. If more energy can be harvested than the system needs, e.g. when the system is in sleep mode, the excess energy is stored in the storage element. When the system wakes up and needs more energy, the PMU uses the stored energy to keep the regulated output voltage stable. The cold start-up function and the maximum power point tracking (MPPT) makes the ADP5092 very efficient with sub microwatt operation losses. After the cold start circuit, the input voltage operating range is from 0,08 V to 3,3 V. The ADP5092 provides a regulated output voltage which can be set from 1,5 V to 3,6 V with a maximum current of 150 mA and also an unregulated output. The VID pin of the ADP5092 is left floated with the effect that the regulated output is set to 2,5 V which is used to power the MCU and the radio module.The unregulated output is connected to the ADP165 low dropout (LDO) regulators which power the ADXL1002 accelerometer and the AD4000 analog-to-digital converter (ADC). The unregulated output is internally connected to the battery voltage, which means that the output voltage changes with the voltage at the super cap. Therefore, the voltage of the battery has to be monitored to check if there is enough energy stored in the super cap to perform a high power consuming measurement and data transmitting process. In this work, a 0,1 F super capacitor with a nominal voltage of 5,5 V is used as a storage element and the charging threshold is set to 4,5 V.

3.3 Sensors for Condition Monitoring

In this work, two different sensors are chosen because of their different characteristics. The goal of this approach is to combine the features to get a better system performance. The mechanical system presented in section 2.1 generates vibrations at frequencies higher than 1 kHz, therefore, the

high-frequency accelerometer ADXL1002 is chosen as an additional sensor to be able to measure high frequencies. The ADXL355 is chosen because of the high sensitivity for lower frequencies. The ISO10816-3 [iso17] standard defines the bandwidth of the measurement equipment for vibration measurement, a frequency range from 10 Hz up to 1 kHz is sufficient but a higher bandwidth can be necessary if the measurement is also used for diagnosis purpose. The ISO 13373-1 [iso02] standard defines a frequency range up to 10 kHz for mechanical purposes. The frequency range of more than 80 % of the available CbM systems and sensors for condition monitoring is less or equal to 10 kHz and only less than 20 % of the sensors or systems are able to measure above 10 kHz. The ADXL1002 with a high bandwidth is a good choice to cover the frequency range up to 11 kHz.

ADXL355: The ADXL355 is a low power MEMS accelerometer with a low noise density and a low 0 g offset drift. The device combines three measurement axes into one package and the integrated temperature sensor also allows temperature monitoring. The power supply range is from 2,25 V to 3,6 V and the current consumption in measurement mode is only 200 μA and 21 μA in sleep mode. The data exchange with a microcontroller can be implemented through an SPI or an I^{2}C interface. The sensor can be used for tilt sensing and platform stabilization or structural health and condition monitoring and many more applications. In this work the ADXL355 sensor is chosen because of the high sensitivity and the low power consumption which makes it suitable for a self-powered condition monitoring system [Dev18a].

ADXL1002: The ADXL1002 MEMS accelerometer is a single axis sensor with very low noise density and a frequency range up to 11 kHz. The sensor has an analogue output and therefore an ADC is needed to convert the analogue signal to a digital value for further processing. The current consumption is 1 mA at 5 V which is five times the current consumption of the ADXL355. For a reliable CbM system a sensor with a high frequency range is essential even if the current consumption is higher. The ADXL1002 can measure accelerations up to ±50 g and is optimized for industrial condition monitoring. To cover three axes with a frequency range up to 11 kHz three sensors are needed and mounted orthogonally on the PCB. Three sensors increase the overall system power consumption but also the reliability of the CbM system [Dev17a].

Analog-to-digital converter: To digitalize the analogue signal from the ADXL1002 an ADC is needed. Two different approaches are possible:

- Internal ADC of the microcontroller:
  The microcontroller has an integrated 12-bit successive approximation register (SAR) ADC. This approach only needs two external resistors for a voltage divider because the output signal from the sensor would exceed the input range of the microcontroller. Another advantage of this solution is the lower power consumption as there are no additional devices needed.

- External ADC:
  This approach has a higher power consumption but gives a better performance. More space on the PCB is needed because of the external ADC and a 1,8 V regulator for the supply voltage of the ADC. There is no voltage divider needed because the supply voltage of the sensor can be used as a reference voltage and therefore the analogue output of the sensor will not exceed the input range of the converter.

Table 3.4: ADC performance comparison

	Internal ADC	External ADC
Integral Nonlinearity Error (INL)	±1,6 LSB	Typ. ±0,2 LSB
Differential Nonlinearity Error (DNL)	-0,7 to 1,1 LSB	Typ. ±0,5 LSB
Dynamic range	74 dB [1]	93,5 dB

1 Ideal Signal to Noise Ratio (SNR)

Most characteristics of a microcontroller's internal ADC are typically not shown in the data sheet. Integral Nonlinearity Error (INL) and Differential Nonlinearity Error (DNL) are defined in the data sheet and in Table 3.4 it can be seen that the external ADC has a better performance than the internal ADC. The SNR, also called dynamic range, is an important characteristic of an ADC. The SNR of the internal ADC is not defined but the SNR of an ideal ADC can be calculated as follows [Kes06]:

$$SNR = n \times 6.02 + 1.76 \, dB$$

As the internal ADC is not ideal the SNR will be lower than 74 dB and would decrease the performance of the signal chain and therefore an external ADC is chosen in this work.

Filter: As the frequencies measured from the test set-up, see section 4.1, are expected to be lower than 5 kHz and the sampling rate is not higher than 32 kHz, a single-pole RC filter with a cut-off frequency of 5,3 kHz is used to filter the signal from the sensor to avoid aliasing [Dev17a].

3.4 Microcontroller

The microcontroller used in this work is the ADuCM4050. It is an ultra low power ARM Cortex M4 controller with a floating-point unit (FPU). The microcontroller has a power supply range from 1.74 V to 3.6 V and a low power consumption so it is suitable for self-powered or battery-powered devices, for example, Internet of Things (IoT), wearable or fitness and clinical devices. The different power modes allow a perfect adaption to the given task and the different digital peripherals offer a wide range of applications. As the sensor node will remain in sleep mode most time, the very low power consumption of the ADuCM4050 in shutdown mode helps to reduce the overall system power consumption. The data exchange with the sensor, the ADC and the radio module is realized through the Serial Peripheral Interface (SPI) [Dev18b].

3.5 Radio Module

The nRF8001 Bluetooth Low Energy Connectivity IC is chosen as a wireless data exchange solution. The chip is Bluetooth Low Energy v4.0 qualified and integrates a radio, a Link Layer and a Host Stack. The simple serial interface (ACI) allows interfacing with a wide range of microcontrollers. The nRF8001 is designed to operate as a peripheral (slave) device which means that only a central (master) device, for example, a phone, can establish a connection. The low

current consumption of 0,5 µA in sleep mode helps to reduce the overall system power consumption because the nRF8001 will mostly be in sleep mode. Only when data needs to be sent the Bluetooth chip will be in active mode and a connection will be established. After the data is sent the connection will be closed and the nRF8001 will be set to sleep mode again. This approach is less power consuming than keeping the connection as radio transmissions are needed to keep the connection, see Figure 3.6. This figure shows the supply current of the radio module, the current peaks indicate a so-called connection event, during this events the processor and the radio unit of the radio module are active and data is transmitted. Even if no data needs to be sent, the current peaks still occur to keep the connection. To reduce the power consumption the time between this connection events, so-called connection interval, can be increased. This has the effect that the throughput is lower because data transmission takes longer. Another option to reduce the power consumption is to implement slave latency, which means that the radio module can skip connection events when no data needs to be send. This effect can be seen in Figure 3.6; the high peaks indicate a connection event where transmissions take place while the lower peaks indicate the skipped connection events. The skipped events can still be seen in the supply current as lower peaks because the microcontroller wakes up from sleep mode but the radio unit is not active and therefore the peaks are lower. For this measurement a connection interval of 48,75 ms is chosen.

One reason for the higher current consumption when the connection is kept are the continous current peaks. Another reason is the idle current between the connection events which is about 2 µA while the sleep current of the nRF8001 is about 0,5 µA [Sem15]. The average current consumption depends on several factors, for example, the sleep/awake ratio or the connection interval. The connection parameters have to be choosen to balance data throughput and power consumption. With the software nRFgo Studio the average current consumption can be calculated for different connection parameters to show how changed parameters affect the current consumption.
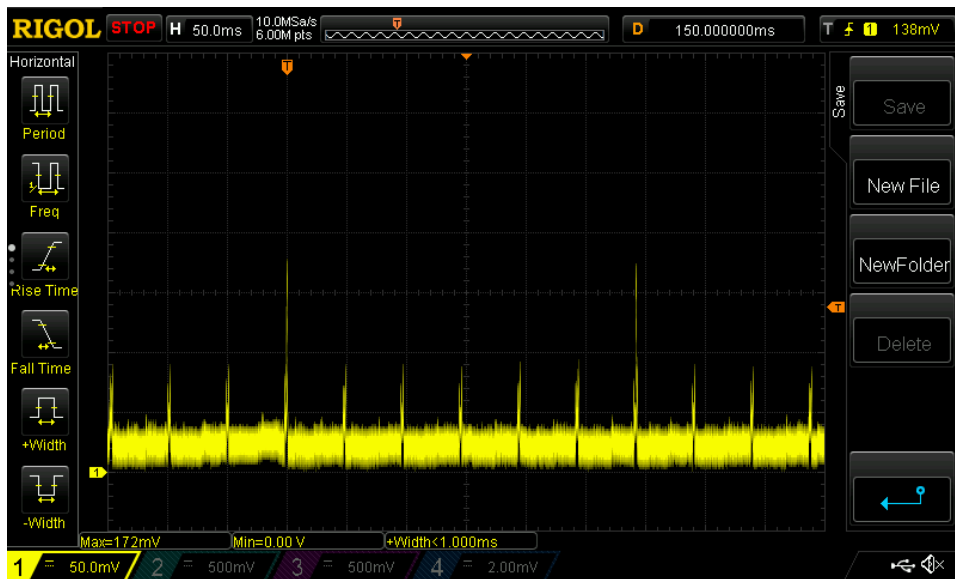

Figure 3.6: Supply current of the radio module to illustration connection events and slave latency

3.6   System Design

This section describes the whole system and the test set-up. The concept of the condition monitoring node developed in this work is shown in Figure 3.7: The TEG converts heat energy into electric energy and the power management unit converts the low voltage into a higher voltage, stores excess energy in the storage element and provides energy to the system. The ADP5092 provides 2,5 V regulated output and an unregulated output voltage which is affected by the super cap voltage. The processing unit is the ADuCM4050 which manages the tasks of the sensor node, it is powered from the regulated output. The ADXL355 accelerometer is powered through a general purpose input/output (GPIO) pin of the microcontroller with the effect that the sensor can be unpowered when it is not needed to save energy; otherwise, the sensor would stay in sleep mode and would continuously consume electrical energy. This approach cannot be used for the Bluetooth chip because the peak current during transmission is too high for the GPIO pin, therefore the nRF8001 is also powered from the regulated output and set to sleep mode when it is idle. The data exchange with the nRF8001 and the ADXL355 is done through an SPI interface. The analogue signal from the ADXL1002 is digitalized by the AD4000 ADC and the digital data is also transferred through an SPI interface to the microcontroller. The ADXL1002 accelerometer and the AD4000 ADC require two different supply voltages: 1,8 V and 3,3 V. The regulated output is used to power the ADP165 LDO regulator which provides 1,8 V power supply for the AD4000. A second ADP165 is powered by the unregulated output and provides stable 3,3 V for the ADXL1002 power supply and the reference voltage for the AD4000. Both LDO regulators can be disabled by the MCU to save energy by only enabling them when they are needed. When the voltage regulators are turned off, the AD4000 and the ADXL1002 are unpowered while the shut-down current for the regulators is typically very low. The voltage level of the super cap is measured to evaluate if there is enough energy stored to perform a vibration measurement and transmit the measured data.
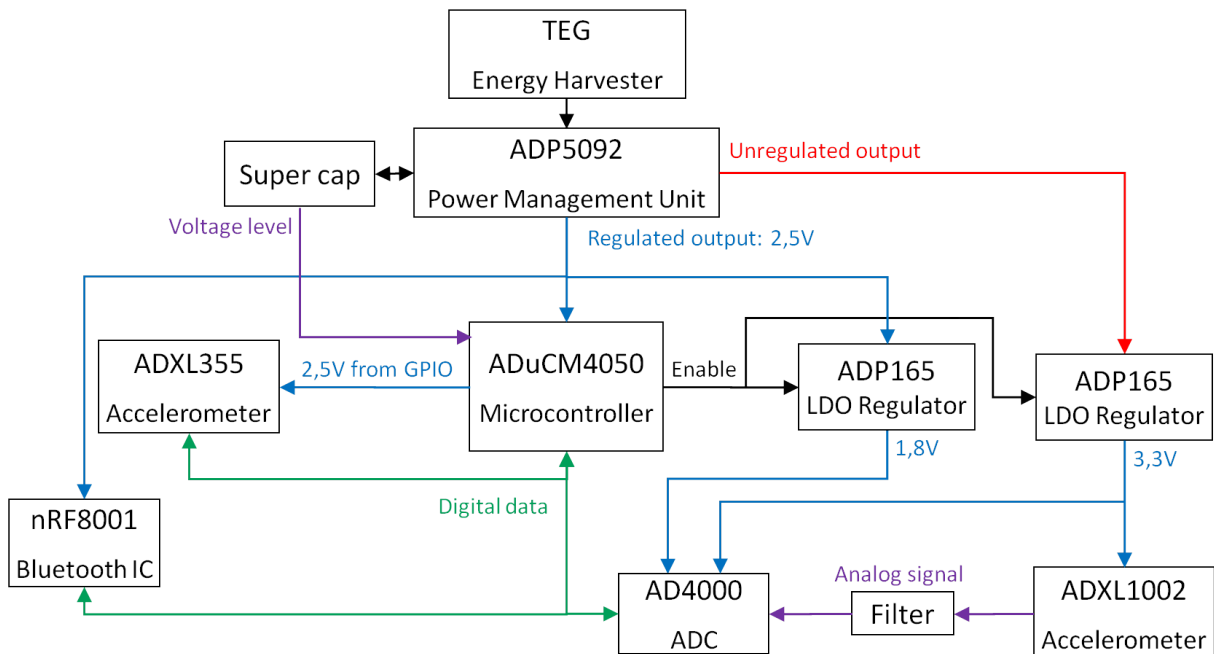

Figure 3.7: Block design of the test set-up

For the test set-up only one ADXL1002 and one AD4000 are used. For a reliable CbM system, three sensors should be used to cover a high vibration frequency range for all three axes. To calculate the correct power consumption the power consumption of one signal chain (ADXL1002 and AD4000) can be multiplied by three and the vibration data of the sensor is sent three times to achieve the same amount of data as it would be with three sensors. The ADP165 regulators are able to provide enough current for three accelerometers and ADCs and therefore no additional regulators are needed.
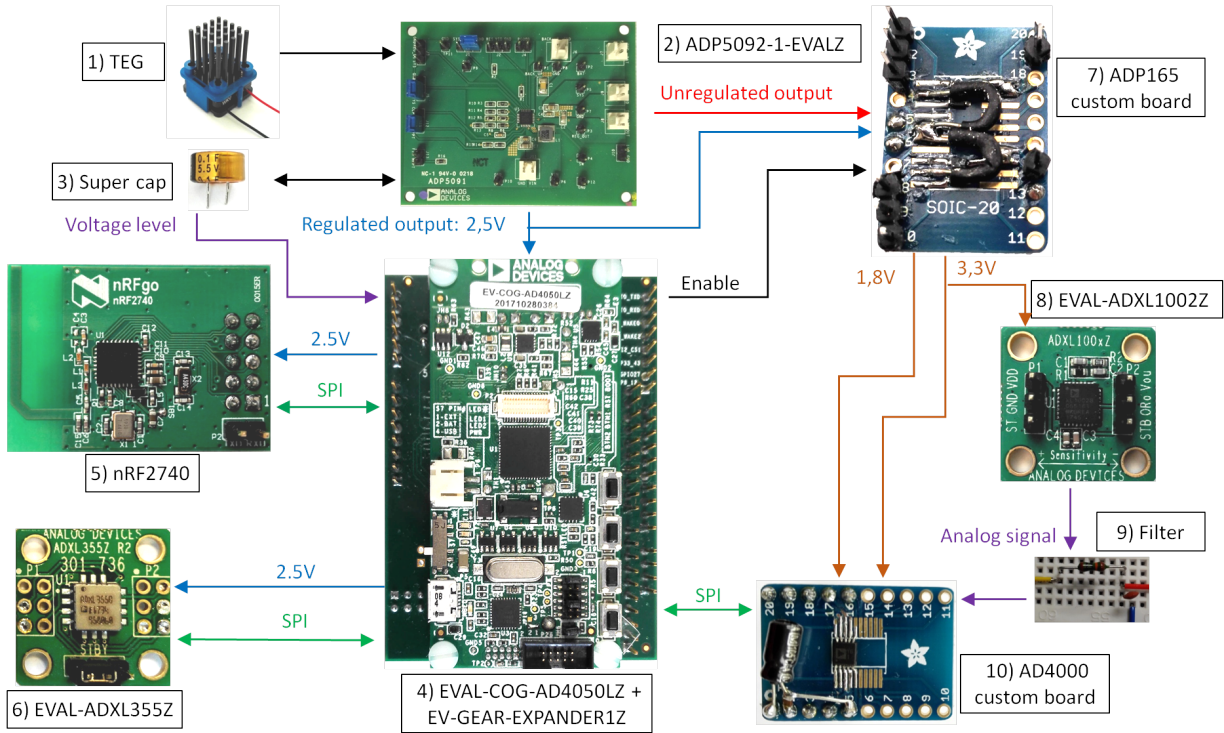

Figure 3.8: Test set-up with evaluation boards

Evaluation boards used for this work:

1. The TEG used in this work is the EHA-PA1AN1-R04, see section 3.1.3 for more details about this device.

2. ADP5092-1-EVALZ: The evaluation board allows an easy evaluation of the device. Replacing resistors of the resistor dividers allow an adaptation of the thresholds and the regulated output can be set by connecting an external resistor.

3. Storage element: A 0,1 F super capacitor with a nominal voltage of 5,5 V is used to store the electrical energy.

4. EVAL-COG-AD4050LZ: The platform is designed for development and prototyping, it allows an easy evaluation of the microcontroller because no external debugger or emulator is needed. The board can be extended with the EV-GEAR-EXPANDER1Z which provides access to all GPIO pins of the microcontroller.

5. nRF2740: The nRF2740 is a radio module with the nRF8001 Bluetooth Low Energy (BLE) chip and a PCB antenna on it. All necessary pins from the chip are accessible via two connectors.

6. EVAL-ADXL355Z: The breakout board is ideal for evaluating the sensor as it is small in size and provides access to the sensors pins.

7. ADP165 board: This is a customized, self-made board because the LDO regulator only require two external capacitors; both LDO regulators are soldered on a breakout board.

8. EVAL-ADXL1002Z: The evaluation board is similar to the ADXL355 evaluation board, it is a small board and all necessary pins are accessible.

9. Filter: A single-pole RC filter as recommended in [Dev17a] is realized on a prototype board.

10. AD4000 board: This is a customized, self-made board for the AD4000 ADC as it only requires one external capacitor and the package can be soldered on a breakout board.

3.7 Application Software

The application software is designed so that the devices are only in active mode when tasks have to be executed and are set to sleep mode when they are finished with it. This saves energy because the power consumption in sleep mode, is much lower than in active mode. When enough energy is harvested the PMU enables the regulated output and powers up the microcontroller and the radio module. The MCU performs some initializations, for example choosing the clock sources or configuration of GPIOs and interfaces. Furthermore, the configuration data is sent to the nRF8001. After the initialization the ADP165 LDO regulators are disabled, the nRF8001 is set into sleep mode, the GPIO pin which powers the ADXL355 accelerometer is set low and the ADuCM4050 is set into hibernate mode. A Real Time Clock (RTC) is configured to wake up the MCU periodically so that the voltage level of the storage element can be measured. If the voltage is too low the MCU is set back to hibernate mode, if the voltage level is above 4,4 V, enough energy is stored and a vibration measurement can be performed. The GPIO pin for the ADXL355 is set to high and data is acquired with it. After the ADXL355 is powered down again the LDO regulars are enabled to power up the ADXL1002 accelerometer and the AD4000 ADC and data is acquired before powering them down again. After the data is measured, the Bluetooth chip is set into standby mode and starts advertising. If a connection is established, the measured vibration data is sent to the analysis device for further processing. Figure 3.9 shows the flowchart of the application software.

Data format of the transmitted data
This section describes the amount and the meaning of the transmitted data. The nRF8001 receives data packets from the MCU and sends it to the analysis device; the maximum packet size is 20 bytes. The data must have some form of identification information because there are two different sensors in the system and each data packet must have a number because the vibration data is sent in several packets. Each packet consists of one byte for sensor and axis identification (ID), one byte which includes the packet number (#) and 18 bytes of data.
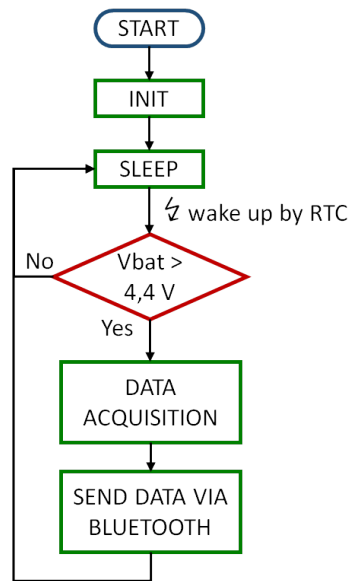
Figure 3.9: Software flowchart

Data measured with the ADXL355

The ADXL355 provides the measured data as a 20-bit value for each axis; each summed up to three bytes. The remaining 18 data bytes contains six measurement results of one axis. When acquiring 1024 samples, 171 data packets need to be sent (1024/6=171) for each axis. Altogether 513 (171×3) data packets have to be sent over the Bluetooth connection for the ADXL355.

Data measured with the ADXL1002

The AD4000 is a 16-bit analog-to-digital converter and the sampled data is summed up to two bytes. The remaining 18 data bytes contain the measured data. Within one data packet nine samples can be transmitted. To transmit 1024 samples 114 data packets are needed (1024/9=114). To send the data of three axes 342 (114×3) data packets are needed.

Table 3.5 and Table 3.6 show the content of a BLE data packet filled with vibration data measured by the accelerometers. Altogether 855 (513+342) data packets, which contain 16,7 KB of raw vibration data, have to be sent over Bluetooth.

Table 3.5: ADXL355 data packet

1	2	3	4	5	6	7	8	9	10	11	12	13	14	15	16	17	18	19	20
ID	#	Data 1			Data 2			Data 3			Data 4			Data 5			Data 6		

ID ... Identification byte
\# ... Packet number

Table 3.6: ADXL1002/AD400 data packet

1	2	3	4	5	6	7	8	9	10	11	12	13	14	15	16	17	18	19	20
ID	#	Data 1		Data 2		Data 3		Data 4		Data 5		Data 6		Data 7		Data 8		Data 9	

ID ... Identification byte
... Packet number

3.8 Power Consumption estimation

The estimated power consumption of each device is shown in Table 3.7 and the average system power consumption as function of the data update rate is shown in Table 3.8. The current consumption of each device is based on the data from the data sheets or is calculated by the software provided from the producer. The average power consumption is calculated for the sleep-active cycle because the initialization has to be done just once at the start up of this sensor node. Figure 3.10 illustrates which devices are active at which time. The blue boxes symbolise the sleep mode of the MCU, the Bluetooth chip and the LDO regulators. The devices which are in sleep mode during the measurement cycle are named under the axis of time for each phase. The green, yellow, grey and red boxes symbolise the active mode of each device named in the box.
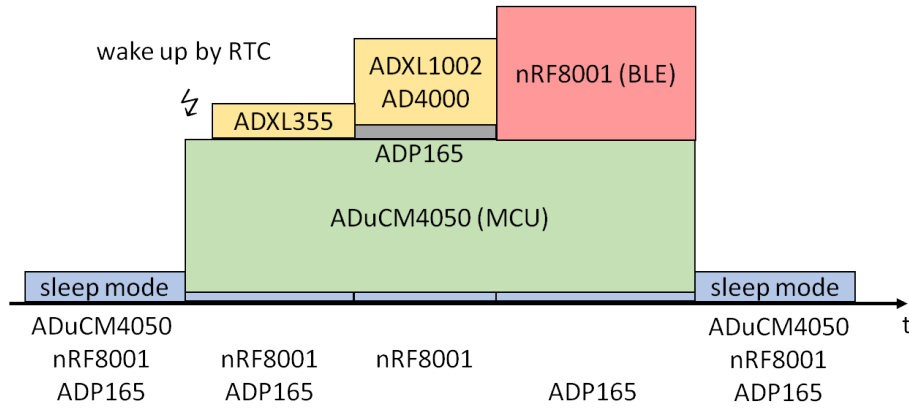

Figure 3.10: Symbolic representation of the active devices during the measurement cycle

Based on the values listed in Table 3.7 the average system power consumption for different data update rates is calculated as follows: The average current consumption for each device is calculated, multiplied by the supply voltage of the device and summed up to the total system power consumption. Depending on the data update rate the average power consumption changes; a shorter update interval means a higher average power consumption, see Table 3.8.

$$I_{\text{average}} = \frac{I_{\text{active}} \times t_{\text{active}} + I_{\text{sleep}} \times t_{\text{sleep}}}{T_{\text{data update interval}}}$$

$$P_{\text{average}} = \sum I_{\text{average}} \times U_{\text{supply}}$$

Table 3.7: Current consumption of each device

Device	Active Current [mA]	Active Time [s]	Sleep Current [µA]
ADuCM4050	3,28 [1]	85 [2]	4,18 [1]
ADP165	0,022 [3]	0,042 [5]	0,1 [3]
ADXL1002	2,4 [4]	0,042 [5]	0 [8]
AD4000	6,66 [6]	0,042 [5]	0 [8]
ADXL355	0,2	0,4 [7]	0 [8]
nRF8001	0,212 [9]	83,4 + 1 [10]	0,5

1 Data sheet

2 Active time of ADXL355, ADXL1002 and nRF8001 summed and rounded up

3 Data sheet; multiplied by 2 because of two LDO regulators in the system

4 Data sheet; multiplied by 3 because of three sensors in the system

5 Calculated for 1024 Samples, f_s is 25600 Hz, T=N/f_s

6 Data sheet: 4 mW at 500 kSPS ; 4 mW/1,8 V=2,22 mA; multiplied by 3 because of three ADCs in the system

7 Calculated for 1024 Samples, f_s is 2560 Hz, T=N/f_s

8 Device is powered off

9 Calculated with nRFgo Studio; 48,75 ms connection interval; 2,3% advertising, 97,7% connected

10 Measurements showed that two connection events are needed to transmit 20 bytes; connection interval is 48,75 ms; the total time is calculated as follows: 2 connection events × 48,75 ms × 855 data packets = 83,4 seconds. 1 seconds for advertising assumed.

Table 3.8: Average system power consumption for different duty cycles

Data update rate	Average System Power Consumption [µW]
12h	29
6h	46
3h	81
1h	219

4 Measurements and Results

The test of the machine condition monitoring sensor node is separated into three parts:

- Measuring vibration data with the sensors and calculating the spectrum to verify the sensors output.

- Evaluating the limits of the TEG.

- Measuring the current consumption of each device, calculating the average power consumption of the sensor node for different data update intervals and measuring the voltage drop at the super cap during data acquisition and transfer.

4.1 Vibration Data Measurement

To verify the sensor's output vibration data is measured and the spectrum is calculated. The test set-up, see Figure 4.1, consists of an arrangement of two vibration motors, each motor has a different rotating speed and both motors are mounted on a board to simulate the vibration of a machine. The accelerometers are also mounted on the board and measure the vibration. The measured vibration data is saved in a file on the computer while the microcontroller is connected to it. The spectrum of the vibration data is calculated and it shows the expected peaks at the dominant frequencies which are equal to the rotating speed of the motors. Table 4.1 shows the characteristics of the used vibration motors.

Table 4.1: Characteristics of the used vibration motors

	Vibration motor 1	Vibration motor 2
Supply voltage	3 V (1,5-3,5 V)	3 V (2-3,5 V)
Supply current	120 mA (30-200 mA)	50 mA (30-60 mA)
Nominal rotating speed	9000 U/min (= 150 Hz)	12000 U/min (= 200 Hz)

The sampling rate for the ADXL355 is 2560 Hz and 1024 samples are acquired. This allows a 2,5 Hz (Δf=f_s/N) frequency resolution of the spectrum. 1024 samples are acquired with the ADXL1002 at a sampling rate of 25600 Hz allowing a frequency resolution of 25 Hz in the spectrum. Measurements showed that if vibration motor 1 is supplied with 3 V the vibration exceeds
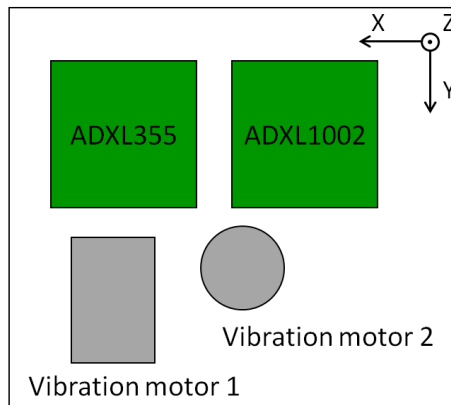
Figure 4.1: Test set-up for vibration measurements

the measurement range of the ADXL355 and the sensor is in saturation. This drawback can be solved by using the ADXL357 accelerometer which has a measurement range up to $\pm 40,96$ g. The ADXL357 is identically to the ADXL355 in terms of dimensions, supply voltage and current consumption and can be used to cover a broader measurement range. For measuring the vibrations with the ADXL355 the supply voltage of vibration motor 1 is decreased with the effect that the acceleration of the vibration doesn't exceed the measurement range of the sensor. Decreasing the voltage also leads to a lower rotating speed of the motor. This effect can be seen in Figure 4.2, which shows the spectrum of the measured vibration of vibration motor 1 in X directions. The peak in the spectrum shows a dominant frequency at 100 Hz and represents the rotating speed which is lower than the nominal rotating speed of 150 Hz. The rotating speed of vibration motor 2 is 200 Hz, Figure 4.3 shows the spectrum of the vibration data of this motor in Y direction with a peak at 200 Hz. To verify the measurements of each motor another measurement is done with both motors turned on. Figure 4.4 shows the spectrum of the vibration data of both motors in Z direction also measured with the ADXL355 accelerometer. The spectrum shows two peaks which represents the rotating speed of both motors. To verify the output data of the ADXL1002 the vibration of motor 1 is measured and the spectrum is calculated, see Figure 4.5. Figure 4.2 and Figure 4.5 show a peak at 100 Hz, this represents the rotating speed of vibration motor 1.
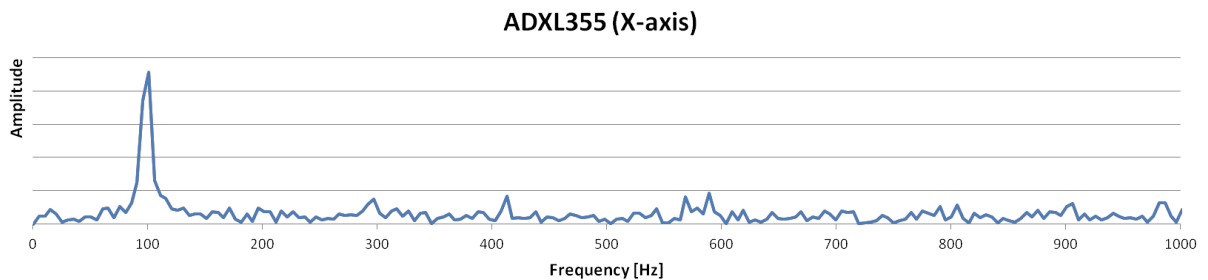

Figure 4.2: Spectrum of vibration motor 1 measured with ADXL355 (X-axis)
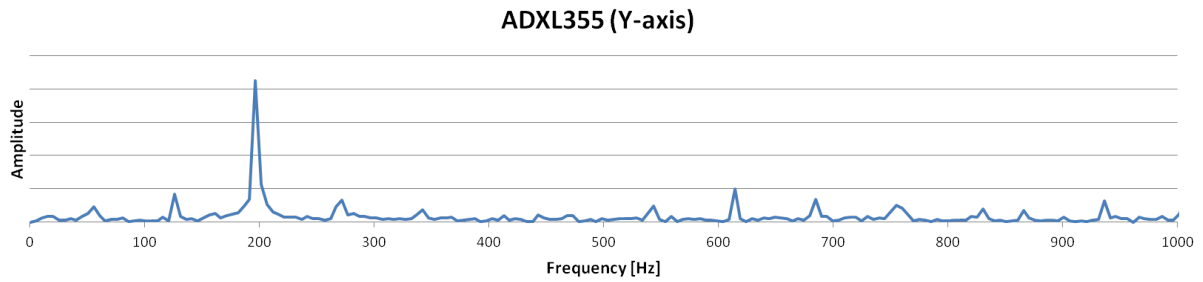
ADXL355 (Y-axis)

Figure 4.3: Spectrum of vibration motor 2 measured with ADXL355 (Y-axis)
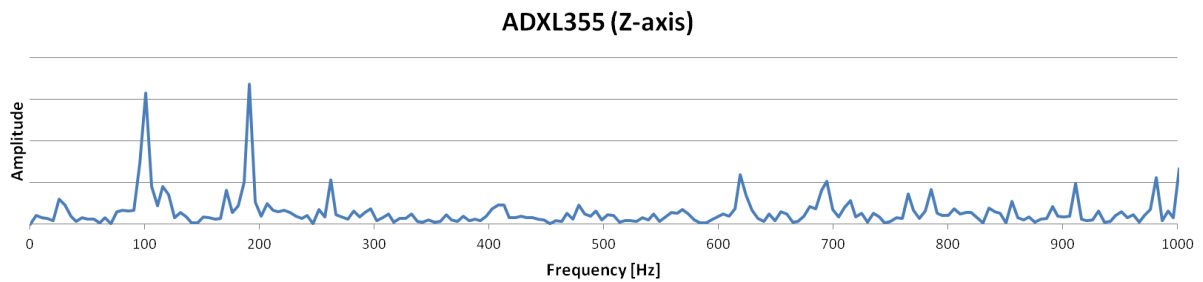
ADXL355 (Z-axis)

Figure 4.4: Spectrum of vibration motor 1 and 2 measured with ADXL355 (Z-axis)
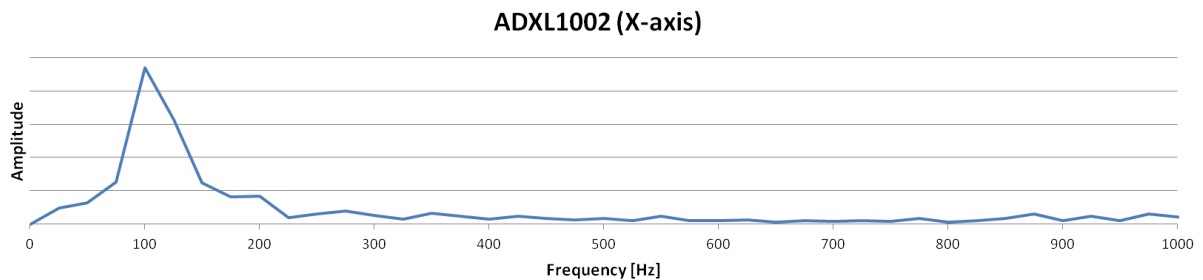
ADXL1002 (X-axis)

Figure 4.5: Spectrum of vibration motor 1 and 2 measured with ADXL1002 (X-direction)

4.2 Evaluating the Limits of the Energy Harvester

The test set-up for the energy harvester consists of a 110 mm x 70 mm 12 W heating foil mounted on the bottom side of a 0,3 mm thick aluminium board and the energy harvester mounted on the top side. The heating foil heats up the aluminium board to simulate the warm surface of a machine. In this section ΔT describes the temperature difference of the hot side of the TEG and the ambient.

Measurements show that the ADP5092 PMU starts operating from an input voltage of 400 mV. A ΔT of about 72 °C is required to achieve an output voltage of 400 mV. After the cold start circuit, the regulator stays in operation for an input voltage from 80 mV to 3,3 V. A ΔT of about 19 °C is necessary to keep the voltage at the super cap at a constant level without any load connected to the ADP5092. This means that the generated energy covers the power consumption of the PMU and the leakage current of the super cap and the voltmeter. The leakage current caused by the voltmeter is about 0,3 µA.

To provide an output power of $200\,\mu\text{W}$ a ΔT of $30.3\,^{\circ}\text{C}$ is required while in [COV^{+}18] a temperature difference of only $10\,^{\circ}\text{C}$ is required to provide the same output power. During the measurements, the heat sink of the used TEG also heated up, a bigger heat sink would help to dissipate the heat from the TEG and this would increase the efficiency of the device.

The measurements show that the used TEG requires a high temperature difference across the device. Other TEGs which require a lower temperature difference are the eTEG HV56 Power Generator from Laird Technologies and the ThermoGenerator-Package (TGP-651) from Micropelt. Both devices are unavailable, Laird Technologies stopped the production of the eTEG HV56 and Micropelt stopped selling the TGP-651 as they only focused on end products with energy harvesters. Analog Devices is developing a chip-scale TEG which can be used to power IoT applications [38].

Figure 4.6 shows the voltage at the super cap as a function of the time for three temperature differences to illustrate the charging process of the super cap. These measurements were started after the sensor node performed a measurement cycle and the data was transmitted, therefore, the voltage at the capacitor dropped, see Figure 4.8. The measurement that has a $26\,^{\circ}\text{C}$ temperature difference was stopped after one hour and the further trend of the voltage was calculated. Table 4.2 lists the time it takes for the voltage at the super cap to reach its charging threshold, this is $4,5\,\text{V}$.
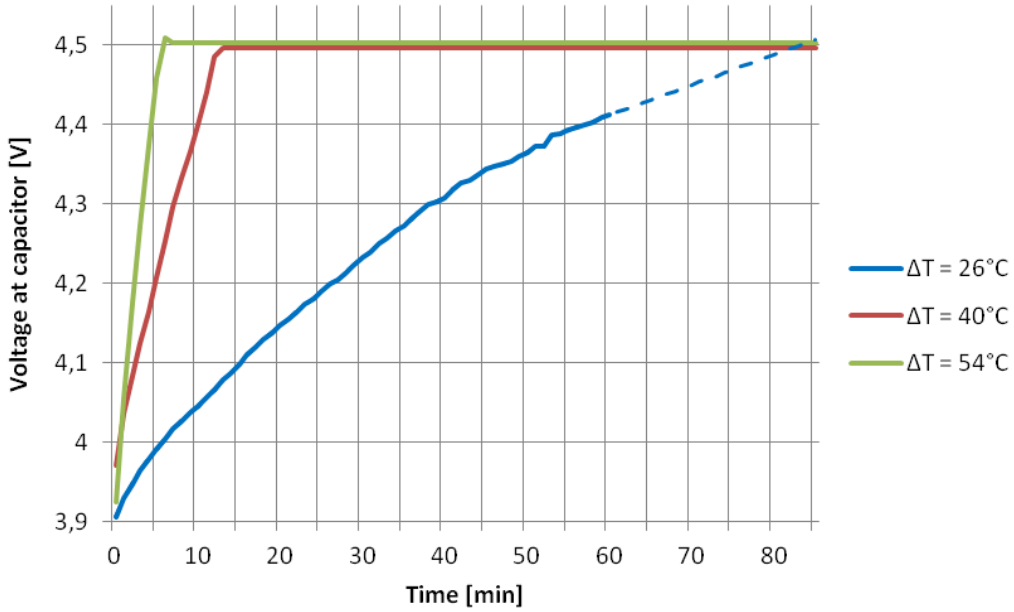

Figure 4.6: Charging process of the super cap

Table 4.2: Characteristics of the used vibration motors

Temperature difference	$\Delta\text{T}=26\,^{\circ}\text{C}$	$\Delta\text{T}=40\,^{\circ}\text{C}$	$\Delta\text{T}=54\,^{\circ}\text{C}$
Time until charging threshold is reached	85 min (calculated)	13 min	7 min

4.3 System Power Consumption

This section shows the measured power consumption of each device of the sensor node and the voltage drop at the super cap during a data acquisition and transmitting process. Table 4.3 shows the current or power consumption of each device and the duration for each task the devices have to perform. The active times of the ADXL355, the ADXL1002, the AD4000 and the ADP165 are higher than shown in Table 3.7 as the start-up time and the time to configure the device is included. Setting the Bluetooth connection interval to 7,5 ms leads to a drastically reduction of the transmitting time with the effect of a reduction of the used energy by the nRF8001, see Table 4.4. This also reduces the active time of the MCU so that it can be set to hibernate mode earlier.

Table 4.3: Measured power consumption of each device

Device and task	Time for task	Current/Power consumption
ADuCM4050: Data acquisition with ADXL355	420,5 ms	4,67 mA
ADuCM4050: Data acquisition with ADXL1002	50,25 ms	4,53 mA
ADuCM4050: Data transfer to the BLE chip	9,48 sec [1]	4,57 mA
ADuCM4050: Data transfer to the BLE chip	13,12 sec [2]	4,57 mA
ADuCM4050: MCU in hibernate mode	-	1,40 μA
ADP165: off	-	20 nA
ADP165 (1,8 V): Total power dissipation [3]	50,25 ms	70,14 μW [5]
ADP165 (1,8 V): Total power dissipation [4]	50,25 ms	155,43 μW [5]
ADP165 (3,3 V): Total power dissipation [3]	50,25 ms	56,62 μW [5]
ADP165 (3,3 V): Total power dissipation [4]	50,25 ms	70,85 μW [5]
ADXL1002: Data acquisition	50,25 ms	768 μA
ADXL1002: Idle	-	0 [6]
AD4000: I_{Ref} (at 3,3 V)	50,25 ms	5,93 μA
AD4000: I_{VIO} and I_{VDD} (at 1,8 V)	50,25 ms	60,92 μA
AD4000: Idle	-	0 [6]
ADXL355: Data acquisition	420,5 ms	191 μA
ADXL355: Idle	-	0 [6]
nRF8001: Data transfer	9,48 sec [1]	2,61 mA
nRF8001: Data transfer	13,12 sec [2]	2,61 mA
nRF8001: Advertising	100 ms − 4 sec	0,576 mA
nRF8001: Sleep mode	-	0,24 μA

1 Time to transmit data of ADXL355 and 1 × ADXL1002
2 Time to transmit data of ADXL355 and 3 × ADXL1002
3 Calculated for 1 × ADXL1002+AD4000
4 Calculated for 3 × ADXL1002+AD4000
5 Calculated as follows: $V_{in} \times (I_q + I_{out})$ - $V_{out} \times I_{out}$ [LLC16] [32]
6 Device is unpowered

Measurements of the whole Sensor Node
The following measurements are done by simulating the power consumption of a sensor node with three ADXL1002 sensors and three AD4000 converters: Data acquisition with the ADXL1002 is performed three times to approximate the power consumption of three sensors and the measured data is sent three times to achieve the same amount of data. The following figures show the

voltage at the super cap (yellow curve) and the regulated output voltage (blue curve).

Table 4.4: Energy consumption of the nRF8001 for data transmitting

Connection interval [ms]	Supply voltage [V]	Supply current [mA]	Time [s]	Energy [mJ]
7,5	2,5	2,61	13,12	85,61
48,75	2,5	0,485	84,24	102,14

Figure 4.7 shows a measurement cycle started when the voltage at the super cap was 4 V. After 14 seconds the voltage at the super cap drops below the shut-down threshold and the regulated output is turned off. After the regulated output is disabled, the voltage at the super cap recovers and increases, the regulated output is enabled again. The MCU starts again and consumes energy so that the voltage at the super cap drops again below the shut-down threshold and the regulated output is disabled again. This behaviour continues until the voltage at the super cap doesn't reach the level to enable the regulated output and it stays disabled. This problem can be solved in different ways:

- Reducing the shut-down threshold so that the regulated output stays on until the measurement cycle is finished.

- Increasing the level to enable the regulated output so that the power-up of the MCU doesn't lead to a voltage drop under the shut-down threshold.

- Starting the measurement cycle at a higher super cap voltage so that it doesn't drop below the shut-down threshold during the measurement cycle, see Figure 4.8.

- Increasing the value of the super cap so that the voltage drop is lower, see Figure 4.9.
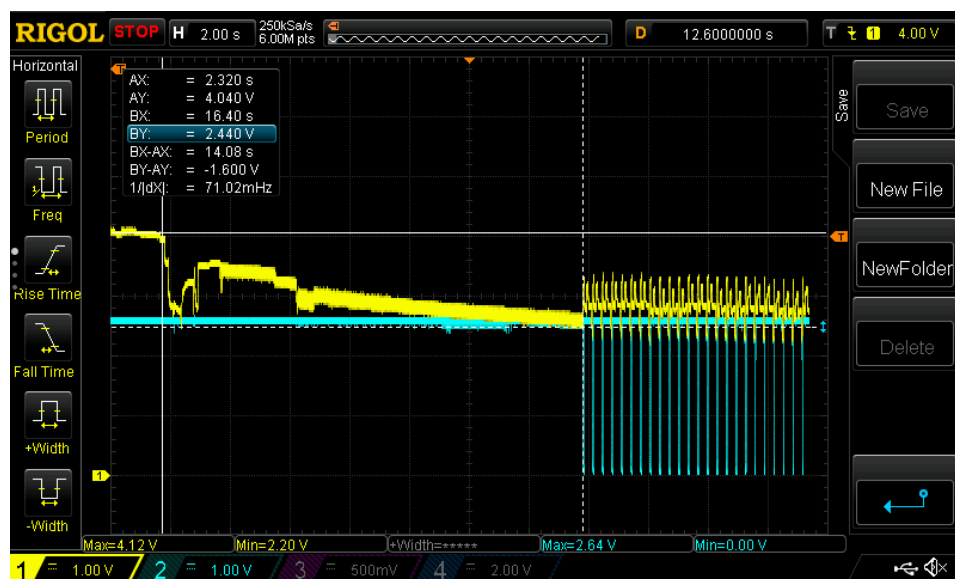

Figure 4.7: To less energy stored in the super cap (0,1 F) for a measurement cycle

Figure 4.8 shows the measurement and data transmitting cycle started when the 0,1 F super cap is charged until the charging threshold of 4,5 V. It shows that there is enough energy stored in the super cap to perform this task and the voltage at the super cap doesn't drop below the shut-down voltage. When the data transfer has finished the voltage at the super cap is 2,9 V. When the system is set to sleep mode again, the change of the current consumption from a few mA to less than 2 μA leads to a voltage increase at the super cap, so-called voltage recovery [SMMA18] [SSS+16] [KSS+14].

Figure 4.9 and Figure 4.10 show the voltage at the super cap when the sensor node is switched on and a measurement cycle is performed. Both figures show that there is enough energy stored in the super cup to power-up the sensor node, do all initializations, perform a data acquisition and send the measured data before the system is set to sleep mode again. Using a bigger capacitor decreases the voltage drop, this is confirmed by following measurements:

- If only a measurement and data transfer are performed with a 0,1 F capacitor, the voltage drops from 4,5 V to 2,9 V, see Figure 4.8.

- The voltage of a 0,33 F capacitor also drops from 4,5 V to 2,9 V if also initializations are performed before the measurement cycle starts, see Figure 4.9.

- Figure 4.10 shows the start-up and measurement cycle with a 0,1 F super cap, the voltage drops from 4,5 V to 2,5 V which is lower than 2,9 V at the 0,33 F capacitor.

The charging process shown in Figure 4.6 is the continuation of the measurement shown in Figure 4.10.
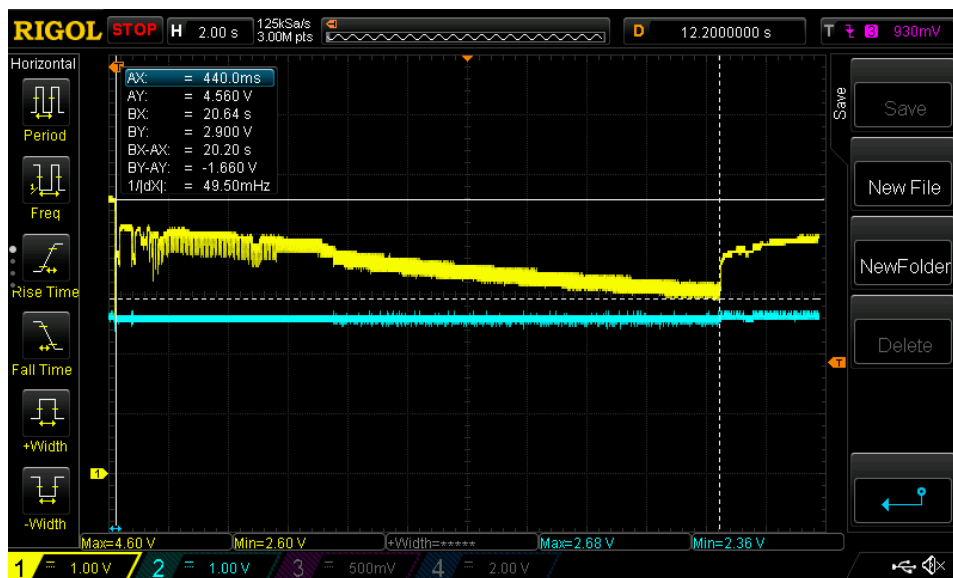

Figure 4.8: Measurement cycle when super cap (0,1 F) is charged to 4,5 V
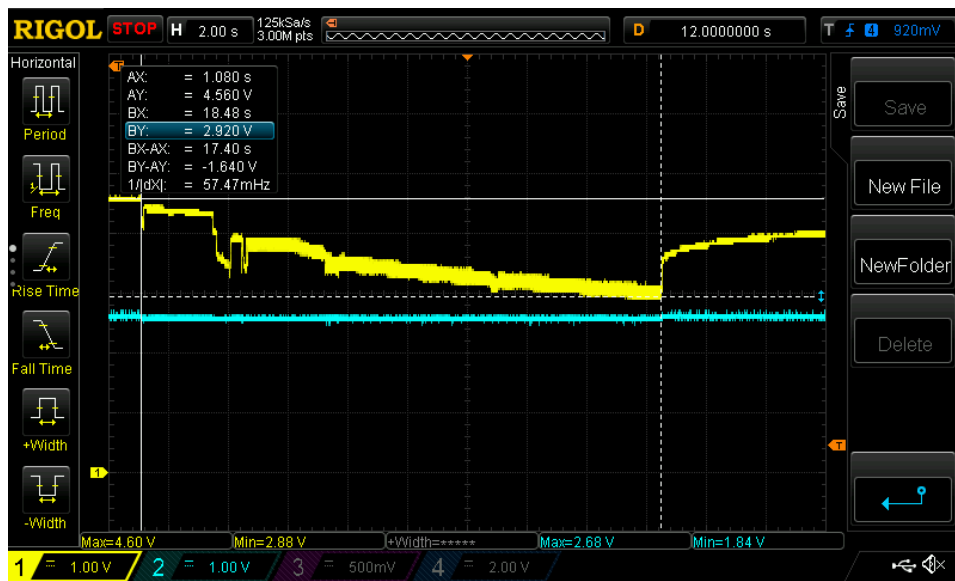
Figure 4.9: Sensor node start-up and measurement cycle with a 0,33 F super cap
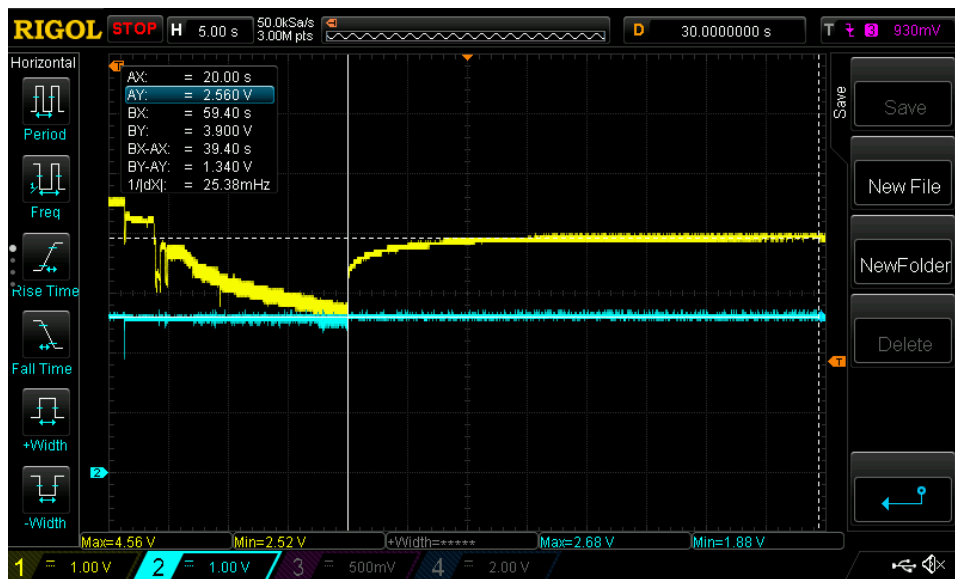

Figure 4.10: Sensor node start-up and measurement cycle with a 0,1 F super cap

4.4 Discussion

The average power consumption of the sensor node is mainly affected by the data update interval, a shorter interval means a higher power consumption. This section describes the trade-off between both parameters. The average system power consumption for different data update intervals is calculated based on the measurements listed in Table 4.3. The calculations are done for the test set-up consisting of one ADXL1002 accelerometer and one AD4000 ADC and also for a system with three ADXL1002 sensors and three AD4000 converters, see Table 4.5. The time from starting advertising until the successful connection establishment cannot be predicted as it depends on

how fast the master device, for example a phone, accepts the connection. Measurements showed that a connection can be established after 100 ms but it can also take up to 4 seconds, therefore, Table 4.5 shows the calculated average power consumption for the best case (100 ms) and the worst case (4 sec).

Table 4.5: Average system power consumption for different data update intervals

	1 × ADXL1002+AD4000		3 × ADXL1002+AD4000	
	Advertising time			
	100 ms	4 sec	100 ms	4 sec
12 h	8,20 µW	9,28 µW	9,72 µW	10,80 µW
6 h	12,30 µW	14,46 µW	15,34 µW	17,50 µW
3 h	20,50 µW	24,82 µW	26,57 µW	30,90 µW
1 h	53,30 µW	66,27 µW	71,52 µW	84,49 µW
30 min	102,51 µW	128,43 µW	138,95 µW	164,87 µW
25 min	122,19 µW	153,29 µW	165,92 µW	197,06 µW
21 min	144,68 µW	181,72 µW	196,74 µW	233,77 µW
19 min	159,48 µW	200,41 µW	217,02 µW	257,95 µW
15 min	200,92 µW	252,76 µW	273,80 µW	325,64 µW
30 sec	5,909 mW	7,464 mW	8,095 mW	9,650 mW

Table 4.5 shows the power consumption difference between a fast connection establishment (column 2 and 4) and a long advertising time (column 3 and 5). For low data update rates, e.g. every 12 or 6 hours, the time until a connection is established doesn't affect the average power consumption much because the sensor node is mostly in sleep mode. If the data update interval is low, a fast connection establishment is important as the advertising time increases the average power consumption.

The power consumption difference of a sensor node with one ADXL1002 and one AD4000 and a sensor node with three ADXL1002 and three AD4000 is small for long update intervals because the whole system is mostly in sleep mode. This difference increases with a shorter data update interval because the sensors and converters have a higher effect on the power consumption.

For an average power consumption of 200 µW in [COV+18] a data update rate of 30 seconds is possible while in this work the update interval increases to 15 or 21 minutes -depending on how many ADXL1002 and AD4000 are installed in the system- when the connection is established within 100ms. For a duration of 4 seconds until the connection is established the data interval is 19 or 25 minutes -also depending on how many ADXL1002 and AD4000 are installed in the system- while the average power consumptio is also about 200 µW. The main reason for the higher data update interval in this work is mostly because of the amount of data which has to be sent and also because of the more power consuming ADXL1002 accelerometer. In this work, the raw vibration data is sent while in [COV+18] only the 50 highest coefficients of the spectrum are sent. For an data update interval of 30 seconds the power consumption is very high -about 5-10 mW- because the sensor node is active for 30-50% of the time.

Table 4.5 shows that a reliable condition monitoring sensor node requires about 10 µW while data is provided twice a day which is sufficient for such a system [Ran11].

5 Conclusions and Future work

A sensor node which measures condition parameters of a machine and sends it to a computer or another analysis device for further processing, trending or archiving is presented in this work. Vibration analysis is chosen as it is able to detect failures earlier than temperature or acoustic analysis and it is a widely used approach for condition monitoring. The used sensors are able to measure vibrations up to $10\,\mathrm{kHz}$ and cover a wide range of possible machine faults. The access to the raw vibration data allows post-processing and analysis of the data in time and frequency domain with the goal of maximizing the chances to detect a machine fault. The sensor node has a low power consumption of about $10\,\mathrm{\mu W}$ when data in X, Y and Z direction is acquired and sent twice a day which is sufficient for a CbM system. The drawback of the used TEG is the need for a high temperature difference across it which limits the area of application. This problem can be solved by using a different TEG which requires a lower temperature difference. To use the harvested energy in an optimized way the developed sensor node provides data as frequently as possible as a dynamic duty cycle is implemented instead of pre-calculated intervals.

The ADXL355 has a measurement range up to $\pm 8\,\mathrm{g}$. While measurements were performed with a test set-up, see 4.1, the accelerometer reached its measurement limit. To cover a broader measurement range the ADXL355 can be replaced by the ADXL357 with a measurement range up to $\pm 40\,\mathrm{g}$. As it has the same power supply range and current consumption the power consumption of the sensor node wouldn't change.

The ADXL1002 can be replaced by the ADXL1003, ADXL1004 or ADXL1005 which were released this year. These sensors have a higher bandwidth than the ADXL1002 so that the sensor node would be able to detect a machine fault which arises at frequencies above $10\,\mathrm{kHz}$.

Nordic Semiconductors recommends replacing the nRF8001 by a newer product as they have a lower power consumption, processing power and usually a lower price.
As a CbM system usually consists of many devices the developed sensor node can be integrated into a sensor network, for example, a SmartMesh IP network [17]. Another network solution which is often used for condition monitoring devices is ZigBee [GWWY18] [ZFMW14] [KJLK10].

Literature

[AAB16]   DE AZEVEDO, Henrique Dias M. ; ARAÚJO, Alex M. ; BOUCHONNEAU, Nadège: A review of wind turbine bearing condition monitoring: State of the art and challenges. In: *Renewable and Sustainable Energy Reviews* 56 (2016), S. 368–379

[BO15]   BHATNAGAR, Vikrant ; OWENDE, Philip: Energy harvesting for assistive and mobile applications. In: *Energy Science & Engineering* 3 (2015), Nr. 3, S. 153–173

[CAP08]   CAP-XX: Good Vibrations Power Wireless Sensors for 'Fit and Forget' Battery-Free Condition Monitoring. (2008), September

[CC08]   CHALASANI, Sravanthi ; CONRAD, James M.: A survey of energy harvesting sources for embedded systems. In: *Southeastcon, 2008. IEEE* IEEE, 2008, S. 442–447

[COV+18] CORNETT, J ; O'GRADY, A ; VOUAILLAT, A ; MICHAUD, J ; MURET, F ; WEATHERHOLTZ, W ; BAI, J ; DUNHAM, M ; RIEHL, P ; CHEN, B [u. a.]: Continuous Machine Health Monitoring Enabled Through Self-Powered Embedded Intelligence and Communication. In: *Journal of Physics: Conference Series* Bd. 1052 IOP Publishing, 2018, S. 012025

[Dev17a] DEVICES, Analog: Low Noise, High Frequency MEMS Accelerometers: Data sheet: ADXL1001/ADXL1002. (2017)

[Dev17b] DEVICES, Analog: Ultralow Power Energy Harvester PMUs with MPPT and Charge Management: Data Sheet: ADP5091/ADP5092. (2017)

[Dev18a] DEVICES, Analog: Low Noise, Low Drift, Low Power,3-Axis MEMS Accelerometers: Data sheet: ADXL354/ADXL355. (2018)

[Dev18b] DEVICES, Analog: Ultra Low Power ARM Cortex-M4F MCU with Integrated Power Management: Data sheet: ADuCM4050. (2018)

[DS08]   DYNYS, Fred ; SAYIR, Ali: Self-Powered Wireless Sensors. (2008)

[EnO15]   ENOCEAN: The True Cost of Batteries – why energy harvesting is the best power solution for wireless sensors. (2015), February

[FHT11]   FAULSTICH, Stefan ; HAHN, Berthold ; TAVNER, Peter J.: Wind turbine downtime and its importance for offshore deployment. In: *Wind energy* 14 (2011), Nr. 3, S. 327–337

[Gol99]   GOLDMAN, Steve: *Vibration spectrum analysis: a practical approach.* Industrial Press Inc., 1999

[GWWY18] GAO, Mingyuan ; WANG, Ping ; WANG, Yifeng ; YAO, Lingkan: Self-Powered ZigBee Wireless Sensor Nodes for Railway Condition Monitoring. In: *IEEE Transactions on Intelligent Transportation Systems* 19 (2018), Nr. 3, S. 900–909

[HVD+15] HELAL, Ibtissem A. ; VUONG, Tan-Hoa ; DAVID, Jacques ; BELLAAJ, Najiba M. ; PIETRZAK-DAVID, Maria: Vibration monitoring based on MEMS accelerometers. In:

Sciences and Techniques of Automatic Control and Computer Engineering (STA), 2015 16th International Conference on IEEE, 2015, S. 240–245

[Inc13] INC., SKF U.: SKF Machine Condition Indicator. In: *SKF Machine Condition Indicator CMSS 200 Reliability meets affordability*, 2013

[iso02] Condition monitoring and diagnostics of machines - Vibration condition monitoring - Part 1: General procedures (ISO 13373-1:2002). (2002)

[iso16] Mechanical vibration - Measurement and evaluation of machine vibration – Part 1: General guidelines (ISO 20816-1:2016). (2016)

[iso17] Mechanical vibration - Evaluation of machine vibration by measurements on non-rotating parts – Part 3: Industrial machines with nominal power above 15 kW and nominal speeds between 120 r/min and 15 000 r/min when measured in situ (ISO 108163:2009 + Amd.1:2017). (2017)

[Kes06] KESTER, Walt: ADC input noise: the good, the bad, and the ugly. Is no noise good noise? In: *Analog Dialogue* 40 (2006), Nr. 02, S. 1–5

[KJLK10] KORKUA, Suratsavadee ; JAIN, Himanshu ; LEE, Wei-Jen ; KWAN, Chiman: Wireless health monitoring system for vibration detection of induction motors. In: *Industrial and Commercial Power Systems Technical Conference (I&CPS), 2010 IEEE* IEEE, 2010, S. 1–6

[KSS⁺14] KUPAROWITZ, Tomáš ; SEDLÁKOVÁ, Vlasta ; SZEWCZYK, Arkadiusz ; HASSE, Lech ; SMULKO, Janusz: Charge Redistribution and Restoring voltage of Supercapacitors. (2014)

[KV86] KOLERUS, Josef ; VARTZ, Wilfried J.: *Zustandsüberwachung von Maschinen. German.* Bd. 3. Expert Verlag Sindelfingen, 1986

[LLC16] LLC, Intersil A.: Zum Verständnis der Linearregler und ihrer wesentlichen Performance-Parameter. (2016)

[Ltd13] LTD, Perpetuum: Vibration Energy Harvesters VEH Technical Datasheet. (2013), October

[MAHH] MONAVAR, H M. ; AHMADI, H ; HASANI, S ; HATAMI, S: Vibration Condition Monitoring Techniques for Fault Diagnosis.

[MR06] MBA, David ; RAO, Raj B.: Development of Acoustic Emission Technology for Condition Monitoring and Diagnosis of Rotating Machines; Bearings, Pumps, Gearboxes, Engines and Rotating Structures. (2006)

[MR10] MURUGAVEL RAJU, Mark G.: Energy Harvesting ULP meets energy harvesting: A game-changing combination for design engineers. (2010), April

[MTPP12] MÁRQUEZ, Fausto Pedro G. ; TOBIAS, Andrew M. ; PÉREZ, Jesús María Pinar ; PAPAELIAS, Mayorkinos: Condition monitoring of wind turbines: Techniques and methods. In: *Renewable Energy* 46 (2012), S. 169–178

[MV05] MARUTHI, GS ; VITTAL, K P.: Electrical fault detection in three phase squirrel cage induction motor by vibration analysis using MEMS accelerometer. In: *Power Electronics and Drives Systems, 2005. PEDS 2005. International Conference on* Bd. 2 IEEE, 2005, S. 838–843

[PPA17] PPA: PPA PRODUCTS Datasheet & User Manual. (2017), January

[Ran11] RANDALL, Robert B.: *Vibration-based condition monitoring: industrial, aerospace and automotive applications.* John Wiley & Sons, 2011

[Sem15] SEMICONDUCTOR, Nordic: nRF8001 Single-chip Bluetooth low energy solution: Product Specification 1.3. (2015)

[SJ15] SHIN, Jong-Ho ; JUN, Hong-Bae: On condition based maintenance policy. In: *Journal of Computational Design and Engineering* 2 (2015), Nr. 2, S. 119–127

[SK17]   SAKHALKAR, Nilashri P. ; KORDE, Pragati: Fault detection in induction motors based on motor current signature analysis and accelerometer. In: *2017 International Conference on Energy, Communication, Data Analytics and Soft Computing (ICECDS)* IEEE, 2017, S. 363–367

[SMMA18] SURAJ, S ; MEJO, AJ ; MURALIDHARAN, MN ; ANSARI, Seema: Self Discharge and Voltage Recovery in Graphene Supercapacitors. In: *IEEE Transactions on Power Electronics* (2018)

[SS09]   SARDINI, Emilio ; SERPELLONI, Mauro: Passive and self-powered autonomous sensors for remote measurements. In: *Sensors* 9 (2009), Nr. 2, S. 943–960

[SSS+16] SZEWCZYK, Arkadiusz ; SIKULA, Josef ; SEDLAKOVA, Vlasta ; MAJZNER, Jiri ; SEDLAK, Petr ; KUPAROWITZ, Tomas: Voltage dependence of supercapacitor capacitance. In: *Metrology and Measurement Systems* 23 (2016), Nr. 3, S. 403–411

[SW17]   SENSOR-WORKS: Bluetooth Wireless Vibration Sensor. (2017), February

[Tec08]   TECHNOLOGIES, KCF: Low-Cost Vibration Power Harvesting for Wireless Sensors. (2008), July

[TEL]   TELEMAQ: VIBRATORY ENERGY HARVESTING MODULES. In: *VIBRATORY ENERGY HARVESTING MODULES*

[TP10]   TAN, Yen K. ; PANDA, Sanjib K.:   Review of energy harvesting technologies for sustainable WSN. In: *Sustainable wireless sensor networks.* InTech, 2010

[TSM+17] THIELEN, Moritz ; SIGRIST, Lukas ; MAGNO, Michele ; HIEROLD, Christofer ; BENINI, Luca: Human body heat for powering wearable devices: From thermal energy to application. In: *Energy conversion and management* 131 (2017), S. 44–54

[TWO+14] TCHAKOUA, Pierre ; WAMKEUE, René ; OUHROUCHE, Mohand ; SLAOUI-HASNAOUI, Fouad ; TAMEGHE, Tommy A. ; EKEMB, Gabriel: Wind turbine condition monitoring: State-of-the-art review, new trends, and future challenges. In: *Energies* 7 (2014), Nr. 4, S. 2595–2630

[WBV+11] WANG, Ziyang ; BOUWENS, Frank ; VULLERS, Ruud ; PETRÉ, Frederik ; DEVOS, Steven: *Energy-autonomous wireless vibration sensor for condition-based maintenance of machinery.* IEEE, 2011

[XWJ08]   XIONG, Xingguo ; WU, Yu-Liang ; JONE, Wen-Ben: Reliability Model for MEMS Accelerometers. In: *Novel Algorithms and Techniques In Telecommunications, Automation and Industrial Electronics.* Springer, 2008, S. 261–266

[ZFMW14] ZHANG, Xihai ; FANG, Junlong ; MENG, Fanfeng ; WEI, Xiaoli: A novel self-powered wireless sensor node based on energy harvesting for mechanical vibration monitoring. In: *Mathematical Problems in Engineering* 2014 (2014)

Internet References

[1] *Accelerometers and Acoustic Emission Sensors from Kistler.* `https://www.kistler.com/en/applications/sensor-technology/test-measurement/tm-acceleration-acoustic-emission/` (Last access: August 29, 2018).

[2] *Acoustic Emission Sensors.* `http://www.fujicera.co.jp/en/product/ae/` (Last access: August 29, 2018).

[3] *ATEX Zone 0.* `https://www.ipu.co.uk/what-is-atex-directive/atex-zone-0/` (Last access: September 24, 2018).

[4] *AVS 2000R unit for continuous monitoring and machine diagnostics.* `http://amcvibro.pl/en/produkt/avs-2000r/` (Last access: September 20, 2018).

[5] *Basic handheld vibration sensor.* `http://www.skf.com/group/products/condition-monitoring/basic-condition-monitoring-products/vibration-measurement-tools/basic-handheld-vibration-sensor/index.html` (Last access: October 30, 2018).

[6] *Batterie-Sammelboxen - Mülltrennung.* `https://www.wien.gv.at/umwelt/ma48/beratung/muelltrennung/batteriebox.html` (Last access: November 5, 2018).

[7] *Batteries and Their Effects on the Environment.* `https://revibeenergy.com/vibrationenergyharvesting/` (Last access: November 5, 2018).

[8] *Condition Based Maintenance (CBM).* `http://www.frtntech.com/wp-content/uploads/2012/05/CBM-Study-Cases-Cost-Analysis.pdf` (Last access: October 10, 2018).

[9] *How Do Thermoelectric Generators (TEGS) Work?* `https://www.marlow.com/how-do-thermoelectric-generators-tegs-work` (Last access: October 25, 2018).

[10] *How Thermoelectric Power Generation Works.* `https://espressomilkcooler.com/how-thermoelectric-power-generation-works/` (Last access: October 28, 2018).

[11] *Ingress Protection Testing.* `https://www.nts.com/services/testing/environmental/ingress-protection/` (Last access: September 24, 2018).

[12] *Lithium-Batterien und Lithium-Ionen-Akkus.* `https://www.wien.gv.at/umwelt/ma48/entsorgung/problemstoffsammlung/lithium-batterien-akkus.html` (Last access: November 5, 2018).

[13] *MAGNET MOUNTING TECHNIQUES FOR MACHINERY VIBRATION MONITORING.* `http://www.pcb.com/contentstore/MktgContent/WhitePapers/WPL_46_Magnet%20Mounting%20Techniques%20for%20Machinery%20Vibration%20Monitoring.pdf` (Last access: October 9, 2018).

[14] *Schallemissionsprüfung - Acoustic Emission Testing (AT).* `https://www.tuev-sued.at/at-de/branchen/industrie-anlagen/zerstoerungsfreie-werkstoffpruefung/schallemissionspruefung` (Last access: September 24, 2018).

[15] *Sensors Database.* `http://www.vallen.de/?id=61` (Last access: August 29, 2018).

[16] *SKF Wireless Machine Condition Sensor - CMWA 8800.* `http://www.skf.com/group/products/condition-monitoring/surveillance-systems/on-line-systems/wireless-systems/wireless-machine-condition-sensor/index.html` (Last access: September 20, 2018).

[17] *SmartMesh IP.* `https://www.analog.com/en/applications/technology/smartmesh-pavilion-home/smartmesh-ip.html` (Last access: November 12, 2018).

[18] *Technical Data Sheet: EHA-PA1AN1-R04.* `https://cdn2.hubspot.net/hubfs/547732/Data_Sheets/EHA-PA1AN1-R04.pdf` (Last access: October 28, 2018).

[19] *Vibration Sensor node (SD-VSN-2).* `https://www.kcftech.com/smartdiagnostics/resources/data%20sheets/KCF_VSN2_data_sheet.pdf` (Last access: September 20, 2018).

[20] *Vibrationsmessgerät / Vibrationsmesser.* `https://www.pce-instruments.com/deutsch/messtechnik/messgeraete-fuer-alle-parameter/vibrationsmessgeraet-vibrationsmesser-kat_10108_1.htm` (Last access: October 30, 2018).

[21] *What is Energy Harvesting?* `http://www.energyharvesting.net/` (Last access: September 25, 2018).

[22] *Wireless monitoring system.* `https://www.oneprod.com/our-solutions/our-products/semi-online-condition-monitoring/semi-online-wireless-solution/` (Last access: September 20, 2018).

[23] *WIRELESS SENSOR NETWORKS.* `http://www.powercastco.com/applications/wireless-sensor-networks/` (Last access: October 14, 2018).

[24] *Zero Power Wireless Sensors Using Energy Processing.* `https://www.mouser.at/storing_harvested_energy/` (Last access: October 28, 2018).

[25] *What is Your Return on Condition-Based Maintenance?*, February 2011. `https://www.nrgsystems.com/blog/what-is-your-return-on-condition-based-maintenance/` (Last access: October 10, 2018).

[26] *Batterien und Akkus*, October 2012. `https://www.umweltbundesamt.de/sites/default/files/medien/publikation/long/4414.pdf` (Last access: November 5, 2018).

[27] Premature bearing failures in wind gearboxes and white etching cracks (wec), March 2013. `http://evolution.skf.com/premature-bearing-failures-in-wind-gearboxes-and-white-etching-cracks-wec/` (Last access: October 8, 2018).

[28] *Energy-Harvester betreiben Herzschrittmacher*, January 2014. `https://www.smarterworld.de/smart-power/energy-harvesting/artikel/105182/` (Last access: September 25, 2018).

[29] *Switching Strategies: Moving to Condition Based Maintenance*, March 2015. `https://www.avtreliability.com/media-centre/white-papers/switching-strategies-moving-condition-based-maintenance` (Last access: October 10, 2018).

[30] *Condition Based Maintenance (CBM) - Optimized Cost Saving*, July 2016. `https://www.petro-online.com/news/fuel-for-thought/13/cmc_instruments_gmbh/condition_based_maintenance_cbm_-_optimized_cost_saving/39608` (Last access: October 10, 2018).

[31] *Lightweight, wearable tech efficiently converts body heat to electricity*, September 2016. `https://www.sciencedaily.com/releases/2016/09/160912132730.htm` (Last access: September 27, 2018).

[32] *Linearregler verstehen und ihre Performance-Parameter kennen. Ger-*

man, March 2016. `https://www.elektronikpraxis.vogel.de/` `linearregler-verstehen-und-ihre-performance-parameter-kennen-a-526662/` `index3.html` (Last access: November 5, 2018).

[33] *Mini-Turbine für energieautarke Herzschrittmacher*, August 2016. `https://www.elektroniknet.de/markt-technik/messen-testen/` `mini-turbine-fuer-energieautarke-herzschrittmacher-133505.html` (Last access: August 15, 2018).

[34] *Schaeffler Global Technology Solutions: Cost Reduction through condition-based Maintenance*, February 2016. `https://www.schaeffler.com/remotemedien/media/_shared_` `media/08_media_library/01_publications/schaeffler_2/global_technology_` `solution/downloads_28/GTS_0003_de_en.pdf` (Last access: October 10, 2018).

[35] *Wearable technology transforms body heat into energy*, September 2016. `http://www.digitaljournal.com/tech-and-science/technology/` `wearable-technology-transforms-body-heat-into-energy/article/474849` (Last access: September 27, 2018).

[36] *Apple, Samsung & Co: Kaum Fortschritte im Kampf gegen Kinderarbeit*, November 2017. `https://www.amnesty.at/presse/` `apple-samsung-co-kaum-fortschritte-im-kampf-gegen-kinderarbeit/` (Last access: November 5, 2018).

[37] *Body Heat Can Be the Source of Power for Wearable Devices*, July 2017. `https://www.powerelectronics.com/alternative-energy/` `body-heat-can-be-source-power-wearable-devices` (Last access: September 27, 2018).

[38] *Powering the IoT with Thermoelectric Energy Harvesting*, 2017. `https://ez.analog.com/b/analog-garage/posts/` `powering-the-iot-with-thermoelectric-energy-harvesting` (Last access: November 14, 2018).

[39] *Sensortechnologien für die Erkennung geringer Anderungen in Maschinenzustanden*, June 2017. `http://www.ni.com/white-paper/52461/de/toc3` (Last access: November 12, 2018).

[40] *AMC Vibration Sensor AVS 2000R User Manual*, 2018. `https://amcvibro.pl/` `wp-content/uploads/2017/09/User-Manual_AVS_27.07.2018.pdf` (Last access: September 5, 2018).

[41] *Batterien – wie umweltverträglich sind sie eigentlich?*, April 2018. `https://www.volvotrucks.at/de-at/news/magazine-online/2018/apr/` `batteries-and-environment.html` (Last access: November 5, 2018).

[42] *Environmental Problems That Batteries Cause*, March 2018. `https://sciencing.com/` `environmental-problems-batteries-cause-7584347.html` (Last access: November 5, 2018).

[43] *Optimization of chip-scale thermoelectric energy harvesters for room temperature energy harvesting applications*, 2018. Presentation from PSMA Inaugural International Energy Harvesting Workshop.

[44] *Taking Batteries out of the Cost Equation for WirelessHART Networks*, March 2018. `https://www.newequipment.com/plant-operations/` `taking-batteries-out-cost-equation-wirelesshart-networks` (Last access: October 15, 2018).

Erklärung

Hiermit erkläre ich, dass die vorliegende Arbeit ohne unzulässige Hilfe Dritter und ohne Benutzung anderer als der angegebenen Hilfsmittel angefertigt wurde. Die aus anderen Quellen oder indirekt übernommenen Daten und Konzepte sind unter Angabe der Quelle gekennzeichnet.

Die Arbeit wurde bisher weder im In- noch im Ausland in gleicher oder in ähnlicher Form in anderen Prüfungsverfahren vorgelegt.

Wien, am 16.11.2018

Philipp Schlögl, BSc.